JGR-Oceans: draft: 4-4-2001

The Detection of Change in the Arctic Using Satellite and Buoy Data

J. C. Comiso

Laboratory for Hydrospheric Processes, NASA/GSFC, Greenbelt, MD 20771

J. Yang, S. Honjo, and R. Krishfield

Woods Hole Oceanographic Institution, Woods Hole, MA

ABSTRACT

The decade of the 1990s is the warmest decade of the last century while the year 1998 is the warmest year ever observed by modern techniques with 9 out of 12 months of the year being the warmest month. Since the Arctic is expected to provide early signals of a possible warming scenario, detailed examination of changes in the Arctic environment is important. In this study, we examined available satellite ice cover and surface temperature data, wind and pressure data, and ocean hydrographic data to gain insights into the warming phenomenon. The areas of open water in both western and eastern regions of the Arctic were found to follow a cyclical pattern with approximately decadal period but with a lag of about 3 years between the two regions. The pattern was interrupted by unusually large anomalies in open water area in the western region in 1993 and 1998 and in the eastern region in 1995. The big 1998 open water anomaly occurred at the same time when a large surface temperature anomaly was also occurring in the area and adjacent regions. The infrared temperature data show for the first time the complete spatial scope of the warming anomalies and it is apparent that despite the magnitude of the 1998 anomaly, it is basically confined to North America and the Western Arctic. The large increases

in open water areas in the Western Sector from 1996 through 1998 were observed to be coherent with changing wind directions which was predominantly cyclonic in 1996 and anti-cyclonic in 1997 and 1998. Detailed hydrography measurements up to 500 m depth over the same general area in April 1966 and April 1997 also indicate significant freshening and warming in the upper part of the mixed layer suggesting increases in ice melt. Continuous ocean temperature and salinity data from ocean buoys confirm this result and show significant seasonal changes from 1996 to 1998, at depths of 8m, 45m, and 75m. Long data records of temperature and hydrography were also examined and the potential impact of a warming, freshening, and the presence of abnormally large open ocean areas on the state of the Arctic climate system are discussed.

1. Introduction

One of the key issues associated with climate change is the role of the Arctic in a warming scenario. Studies based on meteorological station data have indicated that global temperatures have been increasing at the rate of 0.5 °C per century with increases at a relatively high rate in the last 5 years [Jones et al., 1999]. During the last 20 years, the Arctic sea ice cover, as inferred from satellite data, have also been reported to be on the decline at a rate of about 3% per decade [Bjorgo et al., 1997; Parkinson et al., 1999], while submarine studies of the Arctic have also indicated a warming ocean and a thinning ice cover [Morison et al., 1998; Rothrock et al., 1999; Waddams and Davis, 2001].

Because of feedback effects associated with the high albedo of ice and snow, compared to that of open ocean, a climate signal is expected to be amplified in the Arctic [Budyco, 1966; Manabe et al., 1992]. However, the energy exchanges between the ocean, ice, and atmosphere in

the Arctic are poorly understood because of limited surface measurements due to the general inaccessibility of the region. The magnitude and impact of these exchanges, at least in the central Arctic region, were previously believed to be minor compared to those that occur near the marginal ice zones. Recent studies, however, indicate that while the marginal ice zones are indeed regions of intense activities, the inner zones covered mainly by consolidated ice are also sites of significant oceanographic, atmospheric, and biological activities [Aagard et al., 1995, Carmack et al., 1995, Morison et al., 1998]. The significant role of storms in causing profound changes in the vertical structure of ice upper layers of the ocean has also been reported [Yang et al., 2001].

In the Arctic, two general types of water masses have been identified to be dominant: one is the warm and saline Atlantic type generally located in the eastern side, while the other is the cold and fresh Pacific type, generally in the western side. There are also two dominant types of sea ice cover, namely, seasonal and perennial ice, each of which has different impact on the ocean and the atmosphere. In this paper, satellite data are analyzed in conjunction with buoy and other data sets to gain insights into the synergy between the geophysical variables and understand the apparently changing state of the Arctic, especially the Arctic Ocean and it's sea ice cover. The entire Arctic region is studied using satellite passive microwave and infrared data. Some detailed study is done in the western region where the primary buoys are located and where large anomalies were observed. The strategy is to quantify concurrent changes in surface temperature, ice concentration, and ocean parameters and assess the relative sensitivity of these variable to a changing climate system.

2.1 Satellite and Buoy Observations

2.1 Multisensor Satellite Data

Satellite data have previously been used in many Arctic investigations [Comiso, 1990; Gloersen et al., 1992; Kwok et al., 1996; Parkinson et al., 1999]. In this study, we use primarily passive microwave and infrared satellite data because they are the only data sets with long enough record length to provide meaningful interannual variability and trend studies. Satellite passive microwave data provide synoptic coverage of the Arctic surface under day/night and practically all weather conditions. Multichannel brightness temperature data from the Nimbus-7 SMMR and DMSP SSMI have been gridded to a polar stereographic format with a resolution of 25 km by NSIDC. These data are in turn converted to ice concentration maps, using the Bootstrap sea ice algorithm [Comiso et. al., 1997], which provide consistently derived history of the sea ice cover distributions from 1978 to the present. The satellite swath width is about 1600 km and the orbital period is about 110 minutes to enable revisits at most areas in the polar region of as often as 6 times each day. However, only daily averaged data have been archived and this study uses mainly monthly and yearly averages.

Data from the NOAA Advanced Very High Resolution Radiometer (AVHRR) are the primary source of satellite infrared and visible data. At a resolution of 1 km, this sensor provides spatial details that are not possible to obtain from the SSM/I sensor. Also, the visible channel provides information about albedo, and hence the state of the snow cover and the relative abundance of meltponding, while the infrared data provide spatially detailed surface temperature information. However, surface data are available only during cloud free conditions and only during daylight for the visible channels. In this study, we used the GAC data, which have been subsampled at a coarser resolution, because it is the only longterm and continuous data set

available. The primary parameter derived from the GAC data using techniques discussed in Steffen et al. [1992], Comiso [1974], and Comiso[2000] is monthly surface temperature. For convenience in the comparative analysis, the GAC data have been mapped to a polar stereographic grid similar to that used for the SSM/I data but with a resolution of 6.25 km by 6.25 km.

Validations of our interpretation of passive microwave and infrared data have been done through the use of high resolution satellite and aircraft data, including the Synthetic Aperture Radar (SAR) and/or Landsat data (e.g., Comiso and Kwok, 1996) and ship and station data. SAR and Landsat provide complementary information in that SAR operates at a long wavelength and provides surface and subsurface information while Landsat, which is a visible sensor, provides surface information. The retrieved ice concentration products from passive microwave have errors of about 5 to 15% depending on surface condition and season while the surface temperatures derived from AVHRR have errors estimated at less than 3K.

2.2 Surface and Sub-surface Buoy Data

A complete description of the IOEB buoy and its capabilities is given by Honjo et al. [1995] and Kriesfield et al. [1998]. The buoy provides a stable platform from which a consistent and reliable time series of atmospheric, ice, and ocean data can be obtained at its location. The data set is unique in that the buoys provide continuous monitoring of these variables while satellite sensors provide near simultaneous observations of surface parameters that might influence the ocean and ice conditions that are observed from the buoy system. Among the buoy data of interest are atmospheric variables such as air temperatures, wind, and humidity, ice variables such as snow and ice temperatures, and ocean variables such as temperatures,

conductivity, and sigma t. The ADCP vectors also provide information about the direction of currents at different depths.

The trajectories of the two buoys used primarily for this study together with the bathymetry of the Arctic are shown in Figure 1a. One of them, which we call IOEB, was installed on a 4 m ice floe on April 26,1992 at 79.12 N and 132.22 W but due to malfunction, the buoy did not provide good ocean data until April 27, 1996 when it was refurbished. The same buoy was refurbished again on April 11, 1997, with slight modification on the ocean sensor system. The other buoy, called SHEBA IOEB, was installed on September 30, 1997 at 75.08N, 140.92W and collected continuous data up to 1998.

Temperature and conductivity water measurements were acquired by IOEB at depths of 8, 43, 75 m from April 1996 to April 1997, and at 8, 45, and 76 m from April 1997 to January 1998. Hereafter, the three depths will be referred to as 5, 45, and 75 m. Data were acquired internally on an hourly basis but after April 1997 only telemetered data with frequencey of 6.5 per day are available. The SHEBA IOEB buoy provided observations at depths of 65, 105, and 165 m from October 1997 to October 1998.

Temperature and salinity calibrations were performed by the manufacturer of the SeaCats before and after each deployment. In the worst case scenario, the drift of the temperature sensor was less than 0.004 ^{o}C/year and salinity less than 0.02 psu/year. The computation of salinity from conductivity depends on depth. However, no correction to the salinity is applied since the depth uncertainty due to the mooring tilt adds negligible salinity error in typical conditions and less than 0.005 psu at large speed.

In addition to the time series IOEB data, CTD profiles were obtained during buoy deployment operations in April 1996 (150 m depth) and April 1997 (500 m depth) using a Sea-Bird SBE-16 profiler. The precision of these profiles is better than 0.005 °C and 0.01 psu.

3. Seasonal and Interannual Variability in the Sea Ice Cover and Open Water Area

The Arctic sea ice cover goes through large seasonal and interannual variations every year but changes were especially unusual in the Beaufort Sea from 1996 to 1998. A location maps of the Arctic is shown in Figure 1b, which is oriented slightly differently than that of Figure 1a to be compatible with satellite maps. The images in Figure 2 are daily ice concentration maps on October 12th for the three consecutive years. The images correspond to the ice cover during the time of freeze-up and illustrate that at a time when the entire Arctic basin is supposed to be almost totally frozen, as in Octorber 12, 1996, the extent of open water in the region was still substantial in 1997 and even more expansive in 1998. The ice cover in 1996 represents the typical state of theArctic ice cover during this period as observed from satellite data since 1973 [Parkinson et al., 1987; Gloersen et al., 1992]. The areal extent of the open water region in the Chukchi Sea/Beaufort Sea region was about 3.0 x 10^5 km^2 in 1996, more than twice as much at 7.0 x 10^5 km^2 in 1997, and about 9.7 x $10^5$5 km^2 in1998. Such dramatic changes in open water area are remarkable for a number of reasons. First, the open water area is in a region that is usually covered by thick multiyear ice. A replacement of multiyear ice by the seasonal first year ice would make the average thickness of ice in the region substantially less in 1998 than in 1997 and even much less in 1997 than in 1996. Moreover, the predominance of first year ice makes the region vulnerable to ice breakup and the formation of open water in the subsequent summer. Second, a much larger open water area than average (as in 1998) allows for the

absorption of larger amount of solar energy that would cause an increase in the temperature of the mixed layer [Maykut and McPhee, 1995]. Such increase in temperature would in turn inhibit the growth of ice in autumn and winter and accelerates the decay of ice in spring and summer. The process could cause a positive feedback that would lead to thinning in the ice cover. If this process continues, it would lead to the demise of the Arctic multiyear ice cover and cause profound changes in the Arctic Ocean and its environment.

However, we now know that the open water area in the region in 1999 is not any larger than that of 1998. We also know that 1999 is not as warm a year as 1998 (Jones, private communication, 2000). It is thus important that effects of environmental factors in the region are studied in detail. It is known that the Arctic sea ice cover is influenced by periodic changes in atmospheric pressure [Mysak, 1999]. The Arctic ice cover is also not stationary but is very dynamic and undergoes changes in circulation patterns from the dominant anti-cyclonic (clockwise) circulation of the Arctic gyre to a cyclonic (counter-clockwise) circulation [Proshutinsky and Johnson, 1997]. Thus, a large change in open water area in the Beaufort Sea over a three-year period does not necessarily reflect a long term change in the ice patterns.

To illustrate the changing behavior of the Arctic sea ice cover on a longer term basis, monthly ice concentration anomaly maps during September (i.e., at its minimum) for each year from 1981 to 1998 are shown in Figure 3. The color coded images shows where the derived average ice concentrations are anomalously low (redish color) and where they are anomalously high (bluish) in any one year. Areas where the ice concentrations are anomalously very low (dark red) are normally areas of open water during the summer. Changes in areal coverage of the red (and purple) pixels from one year to another thus represent how open water area changes on

a year to year basis. The ice cover during summer minima represents the state of the perennial sea ice cover which consists mainly of ice formed before the summer. The average thickness of the perennial ice is about 3 meters but in heavily deformed areas, the ice can be as thick as 20 meters [Wadhams, 1988]. The red (and purple) pixels are usually areas of high concentration and where much of the multiyear ice in the peripherial regions are advected. During some years, the perennial sea ice cover covers much of Beaufort Sea (e.g., 1983, 1985, 1988, 1991, 1992, 1994, and 1996) while in other years, large open water areas in the region are apparent, including 1990, 1993, 1997, 1998 and 1999. The spatial extent of the anomalies are fully depicted for each year and it is interesting to note that most of the big negative anomalies (reds) occurred in the 1990s.

Quantitatively, the extent and actual areas of the ice cover in the Arctic have been declining as reported previously [Bjorgo et al.,1997; Parkinson et al., 1999]. An updated version of the trend analysis that includes 1978 through 1999 data is shown in Figure 4. The results also complement published reports since the technique used for retrieving ice concentration is different (i.e., the Bootstrap Algorithm as described by Comiso et al.[1997] was used). In Figure 4a, both the monthly ice extent and anomaly distributions are shown with the trend in the anomaly being about –2.8% per decade. A similar set of plot is shown in Figure 4b but with actual ice area anomalies and the trend is slightly higher at about –3%. The difference in trend values can be viewed as the result in the apparent trend in ice concentration during the same period (Figure 4c). Low values in average ice concentration during the summer period are apparent in 1993, 1995, 1997, and 1998. This likely coincide with higher areal extent of meltponding which can cause a bias in the derived ice concentration from passive microwave

data [Comiso and Kwok, 1996]. Thus, decreases in ice concentration may be partly the result of increases in meltponded areas during the summer. In addition to 1993, 1995, 1997, and 1998, the ice extent and ice area were also low in 1990 and 1991. The predominance in the number of low values in the 1990s compared to the 1980s is consistent with the negative trends.

As the ice melts and the ice cover retreats from the land/ocean boundary during the summer, a large fraction of the Arctic Ocean becomes ice-free, as indicated previously, and is directly exposed to the atmosphere. The areal extent of the open water and how it changes is of interest because of its impact on the heat budget and mass balance of ice in the region. To quantify the temporal changes in the open water extent as illustrated in Figures 2 and 3, the Arctic region is divided into an Eastern and Western component, as indicated in Figure 1b. The Western Sector includes data from the Chukchi Sea, Beaufort Sea and the Canadian Archipelago while the Eastern Sector includes data from the Siberian, Laptev, and Kara Seas. The strategy is to be able to quantify separately the open water anomalies in the two sectors which show different variability in Figure 3. The areal extent of open water derived from passive microwave ice concentration data in the Western and Eastern Sectors are shown in Figure 5a and 5b, respectively. A dotted line, drawn by hand, along the approximate maximum extent of open water for each year, except when the maximum appears abnormal, shows an apparent periodicity in the time series. The period of the cycle is approximately ten years but the Western Sector appears to lag the Eastern Sector by about three years. This suggests the existence of a decadal forcing mechanism that propagates around the Arctic. The plots also show surface temperature plots derived from infrared satellite data that shows coherence with the open water areas, as will be discussed in the next section.

In the Western Sector, the maximum open water area, which occurs during late summer, usually fluctuates from about 0.8 x 10^6 km^2 to about 1.2 x 10^6 km^2 . The twenty year record shows low values in 1983 and 1992 and relatively high values in 1987, 1989, and 1995. In 1993, however, instead of a low value for maximum extent, as would be expected in a normal cycle, the extent was abnormally high at 1.5 x 10^6 km^2. Five years later in 1998, the value is even more abnormal at 2.0 x 10^6 km^2. This suggests that although the open water areas usually follows a certain cyclical pattern, the open water area can all of a sudden be very high in one year. It also means that the anomaly is likely not caused by the same forcing that drives the cyclic pattern.

In the Eastern sector, a periodic pattern is also apparent in the maximum extents of open water with the maximum in the 1990s significantly higher than those in the 1980s. In the 1980s, the values range from 1.4 x 10^6 km^2 to 1.8 x 10^6 km^2 while in the 1990s the normal range is from 1.1 x 10^6 km^2 to 2.3 x 10^6 km^2 with dips in 1986 and 1996. Following the pattern, 1995 was supposed to be a year in which the summer open water area is low but it was instead a year when a record extent of open water in the region (2.6 x 10^6 km^2) was observed.

Except for abnormal years, the extent in open water thus follows an approximately decadal periodic pattern. In the Western Sector, an abnormally large open water area was observed in 1993 and an even larger one, the largest in the satellite record, was observed in 1998. In the eastern sector, the extent of open water was substantially higher in the 1990s than in the 1980s. In this sector, however, 1995 stands out as having the largest open water area in the region during the satellite era. It would be of interest to be able to identify the key environmental factor that causes such an abnormal open water phenomenon.

4. Seasonal and Interannual Variability in Surface Temperature

Satellite thermal infrared data currently provide the only synoptic and continuous observation of Arctic surface temperature [Comiso, 1994; Comiso, 2000]. Monthly averaged September temperature anomalies from 1981 through 1999 are shown in Figure 6. These images are especially useful because they provide data not only over sea ice but also over adjacent land and open ocean. Unusually warm areas are indicated by warm (red and purple) colors while unusually cold areas are represented by cold (blue and green) colors. The maps indicate a predominance of anomalously warm temperatures during the 1994 to 1999 period, especially in locations where there are large open water areas during the summer. It should be noted, however, that the anomalously warm areas extend into the land and open water areas indicating that atmospheric warming is at least in part responsible in the observed retreat of the Arctic sea ice cover. This is also a manifestation that the observed ice retreat (and thinning) is only a part of a larger warming phenomenon in the region.

Anomalies on a month to month basis from June to October (except August which is not included because it provide similar information as adjacent months) during the 1996 to 1998 period are shown in Figures 7. The images indicate that the retreat of the ice is not just a summer phenomenon and that changes are also apparent during other periods. The June data indicate that 1996 was a relatively cold year in the Arctic compared to 1997 and 1998. The positive anomalies are also higher in the Central Arctic, Beaufort Sea, and North America in 1998 than in 1997. The July data show that 1996 was again a relatively cold year in the Central Arctic compared with 1997 and 1998. The September data shows even more negative anomalies than in the previous months of 1996 while in Russia, there was a warming in 1997 and a cooling in

Eurasia in 1998. In October, there was a cooling in North American in 1996 and 1997 while the cooling in Eurasia that started the previous month in 1998 continued. It should be pointed out that it was also anomalously warm from June to September in North America in 1996. The negative anomalies in Alaska and Western Arctic in September to October of 1996 were likely responsible for early freeze-up and the relatively low open water in the region in October 12 (Figure 2). Conversely, the persistently warm anomalies in the Western Arctic from June to October in 1998 likely caused the persistence of large open water area in the region during the summer and early autumn of 1998.

Data of surface temperatures over sea ice, with sea ice concentrations greater than 80%, are also plotted together with open water area in Figures 6. The plots show that the peak of the open ocean area distribution lags that of the surface ice temperature peak by about two months. The reason for this is that while peak temperatures are reached in July, the ice continuous to melt until the temperature goes down below freezing temperatures in September. It is apparent that the open water area in both Western and Eastern Sectors are correlated with surface temperature most of the time. For example, when the open water areas were high in 1993 and 1998 in the Western Sector, the average surface ice temperatures in the sector were also relatively high. Similarly, the high open water area in 1995 in the Eastern Sector occurred at the same time as when the average surface temperature was relatively high. It is logical to expect such a relationship since ice grows or decays, depending on surface air temperature but there are exceptions as indicated in the plots.

To quantify the strength of the relationship, yearly ice area is plotted versus yearly surface temperature separately for the Western Sector and the Eastern Sector in Figure 8a and 8b,

respectively. In the Western Sector, the correlation coefficient is 0.61 while regression analysis shows that the ice area decreases by 6.8 ±5.0 x 10^4 km^2/K while in the Eastern Sector, the correlation coefficient is only 0.18 and the regression results show ice area decrease of 5.9±8.4 km^2/K. The results show open water area is better correlated with surface temperature in the Western Region than in the Eastern Region. The reason is likely that of the differences in the environment since the open water in the Western Region is confined and surrounded by land and sea ice while that of the Eastern Region is more directly exposed to an Ocean (i.e., the Atlantic Ocean) and where the influence of the latter on the variability of the open water is likely significant. The correlation coefficients are not very high because the influence on the ice cover by factors other than surface temperature is significant as discussed in the following section.

5. Changes in Wind Patterns and Atmospheric Pressure

Strong persistent wind during the spring and summer can lead to a significant redistribution of the perennial ice cover consisting mainly of multiyear ice. Since the perennial ice cover is much thicker than the seasonal ice cover and more likely to survive the summer, the location of the perennial ice cover is important in terms of open ocean area distribution. Thus, the open water area may be large at the Beaufort and Chukchi Seas during some years because the perennial ice cover is advected to the east while it is not so large during other years because of the dominance of multiyear ice in the region. The same phenomenon applies at other regions like Laptev and Kara Seas. Strong winds can also lead to considerable ridging and compaction and thereby affects the thickness distribution of the ice cover.

To test whether this phenomenon applies to the variability of open water areas from 1996

to 1998, average ECMWF geostrophic winds during four months (June, July, September, and October) around summer and autumn are shown in Figure 9. In Figure 9, monthly wind vectors are shown together with color coded monthly ice concentrations for the same month. Because of constantly changing wind values, monthly averages are used instead of hourly or daily values since the former provides a better assessment of the overall impact of the wind on a periodic basis. It is apparent from the set of images in Figure 9 that wind data indeed show interannual changes that may explain some of the observed spatial distribution of the ice cover. In 1996, the Arctic wind is predominantly cyclonic with intensity and center location varying from one month to another. During the year, strong westerly wind is apparent along the Beaufort Sea from June to August (not shown) changing to northerly in September and back again to westerly in October. In 1997, when there is more open water in the Beaufort Sea than in 1996, anti-cyclonic pattern is dominant in the Arctic basin with strong wind in opposite (easterly) direction in the Beaufort Sea. In 1998, the wind pattern is similar to that of 1997 but are more persistent in one direction and are relatively stronger. It is interesting to note that in July, similar cyclonic patterns are apparent for both 1996 and 1998 near the north pole but near the Beaufort Sea, the winds are going opposite to each other.

Figure 9 indicates that the variability of surface wind was a major factor for the variability of sea-ice concentration and open-water area. This is consistent with previous studies which have emphasized the role of wind-stress driven variations. Sea ice in Arctic Ocean tends to drift in a direction roughly with an angle of 5 to 18 degrees to the right of the geostrophic wind (Thondike and Colony, 1982) and with a somewhat smaller angle to the right of the surface wind wind at 10 meter height. In a state dominated by the cyclonic/westerly wind, as in the

summer of 1996, sea ice was advected from the East Siberian Sea, Chukchi Sea and the central Arctic toward Beaufort Sea, resulting in a build-up of sea ice in the region. Meanwhile, the cyclonic wind can cause divergence of sea ice from the low MSL pressure center because the Coriolis force makes ice to shift to the right side of wind direction. This divergence of multiyear ice from the central Arctic toward the Canadian Basin may have also contributed to the observed high sea-ice concentration and minimum open water in the Beaufort Sea in 1996. Alternatively, anti-cyclonic/easterly wind advects thick multiyear ice from the western region to the eastern region and divergence of sea ice from land-sea boundary toward the central Arctic Basin (due to Coriolis effect) causing large open water areas to be formed in 1997 and 1998. The open-water area in the western section was larger in 1998 than in 1997 partly because the easterly wind was more persistent and generally stronger in 1998. The anticyclonic circulation advects not only sea ice from the western to the eastern region but also transports warmer Bering Sea water to Chukchi Sea where ice melts. The lower ice concentration in 1998 may also be due to the accumulative effect from 1997. After a large openning in the previous summer, the Beaufort Sea region was probably covered by thinner ice before the summer of 1998. This made melting in the region more effective in the summer of 1998. So the combination of these several factors made the open water in 1998 so abnormally extensive.

The changing wind patterns are basically the consequence of changing pressure patterns. To illustrate interannual variability of pressure patterns, yearly anomalies of sea level pressures in the Arctic derived from the ECMWF data are shown in Figure 10. In general, the data is consistent with a decline in surface level pressure previously reported by Walsh et al. [1996]. Like the surface temperature anomalies, the large interannual variability is apparent from the

pressure anomalies. However, the connection of the anomaly patterns with ice concentration and surface temperature data is difficult to make as in the previous discussions since wind directions cannot be inferred directly from the anomalies. What is apparent, however, is that ice was most expansive in the summer (see Figure 3) when the anomalies in pressure are positive around the summer Arctic ice edge (e.g., 1980, 1985, 1987, and 1996). The summer ice cover, on the other hand, tended to be least expansive when the pressure anomalies are negative around the edges (e.g., 1989, 1990, and 1993). Apparent exceptions occurred in 1995, 1997, and 1998 when factors other than pressure may have contributed significantly to the anomalies during these years.

The atmospheric surface pressure and the surface wind in the Arctic region change profoundly on decadal time scales that the surface wind-driven ocean circulation and ice motion can be reversed. Proshutinsky and Johnson (1997) have found that there are two climate regimes in the Arctic coupled atmosphere-ice-ocean system, one with a high atmospheric pressure, anti-cyclonic circulations of surface wind, upper ocean layer and sea ice, and the other with a low pressure center and the reverse of atmosphere, ocean and ice circulations. The time scale for oscillation is about 10 to 15 years. This alternation of high and low sea-level pressure in the Arctic is evidently shown in Figure 10. High pressure anomaly appeared to dominate in early 1980s and late 1990s while the low one was present in mid-1980s and early 1990s. The reversal of the surface wind and oceanic current from one regime to the other undoubtedly have a major impact on the distribution of sea ice. The open water area in the Western Section, as shown in Figure 5, exhibits a 10-year cycle, about the same time scale of the two-regime oscillation discussed by Proshutinsky and Johnson (1997). Very interestingly, the time evolution of the open

water area, marked by the hand-drawn dotted line in Figure 5, is remarkably similar to the index of cyclonic/anti-cyclonic circulation [Proshutinsky and Johnson, 1997; Johnson et al., 1999].

In general, the open water area in the western section is greater in a state of anti-cyclonic wind and ocean circulation when MSL pressure was anomalously high in the central Arctic or over the Beaufort Sea, such as in the case of 1997 and 1998. As we discussed earlier, the sea ice transport from the western to the eastern section increases when the wind is anti-cyclonic. Meanwhile, the Coriolis effect also results in a divergence of sea ice from the land-sea boundary when the wind is anti-cyclonic. The larger opening in the spring and early summer season also creates a favorable condition for a greater heat flux into the oceanic mixed layer in the summer. This positive feedback helps accelerate the melting of sea ice. The solar radiation increases due to lower albedo over the open water than over the ice surface. Indeed, McPhee (1998) has suggested the enhanced solar heat flux was an important factor for large opening in the Beaufort Sea in 1997.

In addition, the opening also exposes the oceanic mixed layer to the direct atmospheric forcing. In events of severe storms, as the one occurred in December 1997 in Beaufort Sea, warm thermocline water was mixed up to the surface and caused considerable melting of sea ice there. As we pointed out earlier, the conditions in 1993 and 1998 in the western section were exceptional. The area of open water was large in these two years despite they being in relative low phases in the decadal oscillation. The MSL pressure anomalies in the summers of 1993 and 1998 were very similar. The MSL was higher over Greenland area. The high pressure extended extended eastward Kara Sea in 1993 and even further to Laptev Sea in 1993. The high MSL pressure also extended westward to the eastern Beaufort Sea in both years. The MSL

pressure was lower north of western Beaufort Sea and Chukchi Sea. The gradient of MSL pressure generated offshore winds in the Beaufort and Chukchi Seas in 1998 and in Chukchi Seas in 1993. These resulted in enhanced sea-ice transport away from the regions and lower ice cover and larger open-water areas in 1993 and 1998. In fact, the distribution of sea-ice concentration anomaly in both years (Figure 3) was consistent with the MSL pressure anomaly (Figure 10). The reason for the high MSL pressure anomaly developed in 1993 and 1998, in the middle of low MSL pressure cycle, remains unknown. But it seems to suggest that there are more than one dominant mode in the MSL pressure variability.

Figure 5 indicates that the area of open water in the eastern section also appears to oscillate at the same 10-year cycle but with a lag of about three years. This is consistent with some previous studies which showed a clockwise propagation of sea-ice concentration anomaly (e.g., Mysak and Venegas, 1998). During the cyclonic phase of the Arctic circulation, sea ice drift is generally directed from the eastern to the western basin (Proshutinsky and Johnson, 1997). This creates a divergence of sea ice in the eastern basin and a convergence in the western basin.

6. Changes in the Arctic Ocean Observed from Buoy Data

Because of general inaccessibility, spatially and temporally detailed hydrographic measurements in the Arctic Ocean are rare if not available. It is fortuitous that CTD measurements up to 500 m were made in April 1996 and April 1997 at two adjacent locations, while buoy hydrographic data at depths of 8, 45, and 75 m were made continuously during the April 1996 through October 1998 period. Although the measurements were not taken at exactly the same spot of the Arctic, the locations (see Figure 1a) are close enough that both should

reflect characteristics of generally similar water masses in the region. Also, the bathymetries are very similar at the two locations. The temperature and salinity profiles, shown in Figure 11a, show large changes in vertical structure from one year to the other. The temperature profile shows a substantial shallowing of the pycnocline from 1996 to 1997 with the temperature maximum of about -1.2° C changing by from –80 m to –50 m. The salinity profile also shows similar change with the average salinity near the surface changing from 30.3 psu to 29.3 psu reflecting significant freshening in the water column close to the surface. Such a change in the characteristics of the Ocean would be profound if it is basin wide.

The difference of temperature and salinity profiles in 1996 and 1997 (Figure 11a) partly reflects of the change of the water mass regime when the IOEB drifted westward from 1996 to 1997. The feature of shallower halocline and thermocline in 1997, especially the structure of temperature maximum at the surface depth of 50m, is commonly found in the western Beaufort Sea and in the Chukchi Sea where the Bering Strait inflow modifies the water-mass structure considerably. The change of the surface wind and oceanic current may have also played a role for the T and S changes. The cyclonic wind associated with the low MSL pressure in 1996 intensified the transport of warmer water from the Bering Sea inflow to the Beaufort Sea and increased sea-ice melting there. In fact, the sea-ice thickness, inferred from IOEB observation of ice temperature, shows clearly a substantial thinning of the ice floe on which the IOEB platform was mounted (Figure 12b). This scenario of warm water advection and ice melting may have contributed to the change from a cooler and saltier upper ocean in 1996 to a warmer and fresher one in 1997.

T-S plots from the IOEB hydrographic data from 1996 through 1998 are shown on a

month-to-month basis in Figure 12, 13, and 14 for depths 8m, 45m, and 75m, respectively. These plots are especially useful for examining seasonal variability and for gaining a better interpretation of interannual changes such as that shown in Figure 11a. It should be pointed out that the buoy is anchored to an ice floe and it is the water column underneath this ice floe that is constantly being sampled by the string of sensors. Since the drift of the ice floe is not necessarily the same as that of the water mass underneath it, some of the changes in the measurements may be associated with the buoy going over a different water mass regime. In Figure 12, data points of potential temperature versus salinity from the entire 8m data set are plotted. The observed values during each month are represented by red data points to provide information about the variability within each month while the time series provides the means to quantify monthly variability. The end points are also labeled A and B that are used as reference data points in the discussion. A large part of the data set varies along a line between A and B indicating linear relationship between potential temperature and salinity at this depth. There are some data points deviating from this line which may be due to external forcing that causes stirring of the mixed layer at the indicated salinity levels.

The line AB basically represents the relationship between the freezing temperature and the salinity value. A large part of the data set varies along this line indicating that the water at this depth was near the freezing temperature in much of this period. There are some data points deviating from this line and they occurred mostly in the summer season (June to August in 1996, and June to September in 1997). This simply indicates the oceanic mixed layer in the summer season was warmed to above the freezing point due to enhanced solar radiation. The only deviation that occurred in non-summer month was December 1997. The warming was due to a

strong and deep mixing with the thermocline water driven by a powerful storm (Yang et al., 2001).

It is apparent that in May 1996, the data during the month are very well defined and close to the highest salinity value. In June 1996, the values were much more variable becoming less saline and warmer at first and then gets colder and more saline after that. In July, the values were basically the same as the previous month but a slight warming is apparent that may reflect the seasonal warming. In August, a slight cooling is observed but salinity is still at its highest values. In September through December, the data points are very confined within the AB line indicating a gradual freshening and a slight increase in temperature. The values are almost constant thereafter from January through April 1997. In May, there is a slight increase in salinity while in June, there is a substantial increase in temperature that again reflects seasonal warming. In July and August, most of the data points are above the AB line indicating significant warming of the water mass. In September, the data points are again mainly along AB and went through considerable freshening and warming in October and November period. In December 1997, the data points slides towards higher salinity along the line AB but at some time period, the values are significantly above the line. It is apparent that the data points are more confined to a certain location in 1996 than in 1997. This may be partly caused by different wind directions in 1996, as indicated in the previous section, compared to 1997. In December 1997, the storm event reported in Yang et al. (2001) is the primary reason for some of the abnormal data points.

The 45 m data in Figure 13, show that there is a lot more variability in the physical properties of the ocean at this depth than at 8m. This greater variability is expected because of the presence of the halocline and thermocline at this depth (see Figure 11a). The large vertical

gradients of temperature and salinity associated with the halocline and thermocline make T and S more sensitive to external forcing such as vertical mixing. The T-S diagrams are shown with labels of A, B, C, and D, which are again used to describe redistribution of data points with time. While a lot of points appear linear and are confined along AB or AC, there are many points that deviate substantially from these lines towards the end of 1997. The salinity and temperature was well defined in April 1996 (not shown but see Figure 11). In May and June, the values are generally more saline and are along the line AB. In July and August, the values are coldest and about the most saline. Then in September through November, the temperatures became siginificantly warmer while salinities were generally less than 31 psu. In December, a general cooling and freshening ensued and this event continued through February 1997. In March through July 1997, the data points are confined along AC, showing basically slight increases in salinity and temperature. In August, some of the data points follow a totally different pattern and confined between C and B but from October through December, the data points each day varied by quite a lot. Again, this later period is associated with a storm in the region as reported by Yang et al. [2001].

At 75 m depth, the IOEB T-S data as depicted in Figure 14, show more defined characteristics of the water mass than at 45 m. In April 1996, the data points during the month are confined to a small cluster (not shown but see Figure 11 as reference). Then from May to June 1996, there was significant warming accompanied by increases in salinity that went on up through September. The values for temperature and salinity then became very well defined in October 1996 through July 1997. After that, the data indicate increasing temperatures and slight freshening up to November 1997 but in December 1997, the data show high salinity but very

variable temperature. The latter indicate that effect of the reported storm [Yang, 2001] was at least as deep as 75 m.

The IOEB data show generally a warmer and fresher water in 1997 than in 1996 near the surface at 8 m, while at 45 m and 75 m, the water was warmer and more saline. These results are consistent with the results from the more detailed CTDs in April 1996 and April 1997. The fresher water near the surface is suggestive of more ice melting in 1997 compared to 1996. Note that the salinity profiles for 1996 and 1997 crosses at about 40 m in Figure 11a, which is the approximate depth of one of the buoy measurements. The warmer water may be related to the larger open water area in 1997 that likely caused an increase in the solar heating of the mixed layer. IOEB ice depth data are compared in Figure 11b for 1996 and 1997, and it is apparent that the ice thickness decreased substantially from one year to the other.

It should be pointed out that the IOEB buoy was mainly in deep water (>3000m) during the study period but there were times when it went to a slightly shallower water (1000-2000m) as as in July 1997. The water mass is usually sensitive to the presence of a shelf slope and some of the changes observed during the period may be associated with such change in bathymetry.

Since the IOEB went to shallow waters in 1998, the ocean measurements from this sensor are more difficult to interpret as part of the time series. For completeness, the results from the SHEBA IOEB from October 1997 through September 1998 are shown in Figure 15. The only data that can be compared directly with those of Figures 12-14 are those at 65 m depth. This buoy was deployed at generally the same water mass region as that of IOEB but the characteristics of the water may not be exactly the same and the measurements at 65 m depth may not match those at 75 m for the other buoy especially near the pycnocline. The TS data for

the 12 month period at 65 m are shown in Figure 15a. Significant activity occurred in January through March 1998 but overall, the change was towards a more saline and colder water. Comparing these plots with those of Figure 14 (for 75 m measurements), it is apparent that the data points along AB in Figure 16a correspond to data points along CD in Figure 14 during the period of overlap in October and November 1997. A warming episode occurred at 75 m (Figure 15) in December 1997, but this event was not observed in the 65 m data (Figure 15a) until January to March 1998. It should be pointed out that the buoy went through significant change in bathymetry during these periods (see Figure 1a). Generally, the water was cooler and slightly more saline in 1998 than 1997 (and 1996) at this depth.

To get an idea about temporal changes deeper in the ocean, T-S plots at a depth of 165 m are generated from SHEBA IOEB data and presented in Figure 15b. From October 1997 to January 1998, the data points are basically confined in the same cluster. From February through May, 1998, the water mass apparently became warmer and more saline, with the data points migrating from location A to location C along almost a straight line. Again, at about February, the buoy went through significant change in bathymetry (Figure 1). From June through September 1998, the data points are in a different cluster that might represent a different water mass regime confined along CB. During this period, the water mass was warmer and more saline than the October 1997 data. It is, however, important to note that from October 1997 to September 1998, the buoy has been advected by hundreds of kilometers.

The albedo over sea water is known to be much smaller than that over the ice surface. Solar radiation through open water areas in the summer is a major source of heat for the Arctic Ocean mixed layer (Mykut and McPhee, 1992). So the air-sea heat is important for variability of

the sea-ice concentration. We speculate that the wind forcing plays a more direct role in the spring and early summer by openning up the ice. The radiation-albedo feedback provides an additional positive feedback by warming the mixed layer and accelerating ice melting.
In 1996, for instance, the ice concentration was high in Beaufort Sea in all summer months due to the presence of cyclonic wind. While solar radiation into the ocean was suppressed during this year, anti-cyclonic wind opened up the ice and set a very favorable condition for enhanced solar radiation into the water in 1997 and 1998.

Heat flux associated with oceanic dynamics, such as advection of warm water and vertical mixing is another factor needed to be considered. The Beaufort and Chukchi Seas are known to be strongly influenced by the inflow of Bering Sea water which is considerably warmer than the surface water in the Arctic. This warmer water was evident in temperature profile shown in Figure 11a at the depth of 40m. This warmer Bering Sea water, sitting just 30-40m below the surface, is a large reservoir of heat that can have profound impact on the heat content in the mixed layer.

An example for this occurred in December 1997 when a strong storm forced a deep mixing that brought up this warm water to the surface and melted sea ice considerably in the vicinity of IOEB (Yang et al., 2001). It is also interesting to note that the strong alongshore wind in the Beaufort Sea in 1997 and 1998 may have also forced upwelling along the coast which could be an effective way of bringing warm water to the surface. The wind condition in 1996 was not favorable for upwelling.

7. Long Term Trends in Surface Air Temperatures and Ocean Hydrography

It would be of interest to assess how the observed trends in temperature and ice cover, as

well as ocean hydrography compares with trends from much longer time series data. Using station data with record lengths of 100 years (or more) in the Arctic located >50° N, the monthly anomalies are shown in Figure 16a. Linear regression of the data points yields positive trends in surface air temperatures of about 0.08 °C per decade. This is significantly higher than that of global averages but significantly lower than the 18-year record (0.38 °C per decade) from the same stations. The corresponding 18 year satellite data over the entire sea ice cover yielded an even higher positive trend of 0.44 °C per decade. The satellite data do not have the same measurement accuracy as the station data. It should be pointed out, however, that long term temperature data sets in the Central Arctic are basically non-existent and most of the stations with temperature records of 100 years or more are but a few, located mainly in Europe, and Northern Russia. Where there is station data, the satellite data compares very well with station data. Figure 16a also show the 5-year running mean of the 100-year temperature record showing significant fluctuation but consistency with the trend line. A power spectrum plot from a Fourier analysis of the 5-year running mean is shown in Figure 16b and indicates peaks at about 11.8 and 8.6 years. These peaks are close to the 10 year periodicity observed from the open water distribution as discussed earlier.

To gain additional insight about long term changes in the characteristics of the ocean in the region, available ocean temperature and salinity data in the Beaufort Sea have been assembled and are used to depict the recent trend in water mass properties at 5 depths (10, 40, 70, 110 and 160 m). This was done through comparison with the Environmental Working Group (EWG) optimally-interpolated hydrographic atlas of the Arctic Ocean. Synoptic air, ice and ocean interactions may cause significant variations in hydrographic properties in the surface

layer of the ocean causing short-term bias in individual hydrographic measurements at any discrete time. Consequently, only data sets in which the time series of profiles had frequent measurements made for several months were analyzed. In the Beaufort Sea, these consist of ice camp data from ice island T3 (1958 and 1965-66), Arlis (1960-61) and AIDJEX (1975-76), and buoy data from six SALARGOSs (between 1985 and 1993) and two IOEBs (1996-98). The frequency of the ice camp measurements is generally two per day or less, while the buoys obtain data ten times more frequently, which makes the later data sets more statistically robust. In addition, errors associated with the raw measurements improved from perhaps 0.1 °C and 0.03 ppt before AIDJEX, to ± 0.03 °C and ± 0.03 psu in salinity during AIDJEX, to stated accuracies as good as 0.02 °C/yr and 0.001 S/m/month (psu) in the instrumentation of the buoys.

The ice camp and buoy observations are roughly bounded by latitude from 72° to 80° N and 30° to 170° W, but occupy different periods in time and space between 1958 and 1998. To study trends in the ocean variables, anomaly time series were created by removing seasonal variations on a station-by-station basis using the spatially interpolated climatologies, called EWG, at the corresponding grid point for either summer (June through November) or winter (December through May) seasons. The EWG climatology is constructed from US and Russian data obtained between 1948 and 1993 from drifting stations, icebreakers, and drifting buoys, and contains average temperature and salinities for winter and summer seasons, with a horizontal resolution of 50 km, and vertical spacing of 10 m. While the atlas provides a long-term 3D estimate of hydrographic properties, plots of the station distribution by decades clearly show that the greatest spatial coverage in the Canada Basin was primarily from Russian data in the 1970s. The time series of anomalies are then averaged by summer or winter producing 40 seasons of upper ocean

hydrographic anomaly determinations as shown in Figure 17. The statistical errors in the seasonal means are generally less than 0.1 °C and 0.25 psu, except for the earliest data prior to 1970, which are not included.

The hydrographic data from five AIDJEX ice camps show good consistency with the EWG climatology in 1975-76, displaying only a few temperature anomalies greater than 0.1° and a single salinity anomaly greater than 0.5 psu (all in the summer mixed layer). SALARGOS buoy data between 1985 and 1989 also agree with the EWG climatology, except for elevated temperatures in one, which are associated with high statistical error. After 1989, however, significant freshening in the mixed layer and warming in the upper halocline are observed. SALARGOS buoys indicate that the season-average salinity at 10 m is 0.5 to 0.6 psu less than the EWG between 1990 and 1993. IOEB buoys follow the trend in 1996 and 1997, and detect anomalies increasing from 1.0 to 1.5. Concurrently, temperature differences at depths of 70, 110, and 160 m increase by 0.2 to 0.4 °C in 1990, but recede in 1992 and 1993. From summer 1996 through winter 1998, the temperature anomalies at 70 m again increased by 0.2 to 0.4 °C, but at 110 m, the temperature anomaly receded in the winter of 1997 to 0.1 °C between high values of 0.3 °C in 1996 and 0.6 to 0.7 °C from 1997 to 1998. This indicates a significant decrease in mixed layer density and an increase in stratification after 1989. While the upper halocline warms, the near-surface temperature elevation above freezing remains nearly constant, presumably due to surface processes.

These computations indicate that the AIDJEX stations in 1975-76 and SALARGOS buoys in 1985-89 show the least variation from the EWG climatology at all depths, which is consistent with the EWG sampling bias in the 1970s. On the other hand, a statistically significant

freshening of the near-surface salinity and elevation of the upper halocline temperature in the central Beaufort Sea is indicated beginning after 1989, confirming other evidence by Melling (1998), Newton and Sotirin (1997), and McPhee et al. (1998). Temperatures at 70 and 110 m show a significant increase of 0.7 °C over the climatology, while mixed layer remains near freezing. The timing is consistent with the large increase in sea-ice melt reported by MacDonald et al. (1999), and could be related to the cyclonic Arctic Oscillation sea level pressure pattern (Thompson and Wallace, 1998) and/or reported shift in the upper ocean circulation regime (Proshutinsky and Johnson, 1997). Significant freshening anomalies at 10 m peak in summer 1992 and in winter 1997, with the maximum value exceeding 1.5 psu in 1997. These peaks appear to precede peaks of anomalously low ice concentration by about one year, and also lag changes in transport through the Bering Strait (Roach et al., 1995) by about 3 years.

8. Discussion and Conclusions

Available sea ice, ocean, and atmospheric surface data have been used in this study to gain insight into the current state of the Arctic climate system. The synergy of different geophysical observable in the Arctic region is apparently very strong. The retreat of sea ice from 1996 to 1998 is shown to be coherent with warming episodes in both the atmosphere and the ocean in the region and with changing wind and pressure patterns. Detailed CTD measurements one year apart in approximately the same water mass region also shows a freshening and a warming from 1996 to 1997. This is compatible with more melted ice and warmer temperatures in 1997 than in 1996, as suggested by the other data sets.

The distributions of open water in the Western Sector and Eastern Sector of the Arctic have been quantified separately to better understand the ice dynamics and its circulation patterns.

The open water distributions are surprisingly periodic, with approximately decadal variability but with the peaks in one sector lagging those of the other by about three years. This suggests that the variability is driven at least in part by an atmospheric forcing likely associated with the Arctic Oscillation and the North Atlantic Oscillation (Mysak, 1999). Such periodic variability is interrupted only by the big anomalies like those in 1993 and in 1998 in the Western Sector and in1995 in the Eastern Sector. It is actually these big anomalies that have caused the negative trends in ice cover and positive trends in surface temperatures in the last two decades, especially because the anomalies tended to be higher and more prevalent in the 1990s than in the 1980s.

The value of having spatially detailed surface temperatures provided by satellite infrared data is apparent. These data enable assessment of regional effects of warming and the spatial scope of the anomalies that usually extend beyond the sea ice cover boundaries. A good example is the warming phenomenon in 1998, which may have caused the largest area of exposed water in the Beaufort Sea region. The anomaly was found to be very large indeed in the Western Sector and in North America, but in some other areas, like Russia and the Laptev Sea, there was actually cooling going on. This is indicative of the complexity of the Arctic climate system and the difficulty of making accurate interpretations of available climate data.

The changing wind patterns has also been shown to be a factor affecting the ice variability. The period from 1996 to 1998 shows a change from cyclonic to anti-cyclonic wind vectors that may have facilitated the formation of large area of open water in the Beaufort Sea during the period. The large open water area was partly due to mass transport of multiyear ice from the Western Sector to the Eastern Sector. The anti-cyclonic wind is also the favorable direction for transporting some of the ice floes to the warmer part of the Arctic Ocean, like

Chukchi Sea, where they melt. The anti-cyclonic wind also forces divergence of sea ice from the land-sea boundary toward the central Arctic Basin. The prevailing cyclonic wind also forces upwelling along the boundary. Because the thermocline in the Arctic Ocean is very shallow, the wind-driven upwelling can be effective for upward heat flux to the mixed layer. When ice cover is opened by wind and oceanic current, solar radiation increases and provides a positive feedback to further reduce ice covering.

The role of the Arctic Ocean on the changing Arctic climate is still poorly understood because of lack of spatially detailed and comprehensive ocean data. However, available data show new insights into the state of the ocean during recent years. During the warming episode in the Western Arctic from 1996 to 1998, continuous sampling of the water temperature and salinity in the region was made by IOEB and the results show a warming and a freshening in the upper part of the water column. Detailed CTD hydrographic measurements in April 1996 and April 1997 in approximately the same area in the central Beaufort Sea show a shallowing of the pycnocline from about 80 m to 45 m, a change in salinity of the upper 30 m layer from 30.2 psu to 29.2 psu while the temperature increased from –1.55 to –1.61 °C. These changes in the ocean are significant and suggest an important role of the ocean in the changing Arctic environment. Available historical data from 1957 to the present indeed show that the anomalies in temperature and salinity in 1997 and 1998 were rather unusual.

This study shows that much of the observed trends in the ice cover and surface temperatures are caused by big anomalies in surface temperature, ice concentration, wind and pressure. It is apparent that the anomalies in the 1990s were higher than those of the 1980s. Underneath these anomalies, however, is a decadal variability in many parameters that appears to

be driven by an atmospheric wave that takes about 3 years to propagate from the Western Sector to the Eastern Sector of the Arctic. Some profound changes may have been occurring in the Arctic during the last decade as a result of the big anomalies. The changes, however, are mainly regional and basically nonlinear and it is important to note that the natural decadal variability and the changing wind patterns are integral parts of the variability. A longer data set and more sophisticated analytical tools are needed to improve confidence in the trend results.

Acknowledgements: We would like to acknowledge with gratitude the programming and analysis support provided by Robert Gerstein of SSAI and Larry Stock of Caelumn Research Inc. This project was supported by the NASA Polar Program and the NASA EOS Project.

References

Aagaard, K., et al., U.S., Canadian researches explore Arctic Ocean, *Eos Trans. AGU.* 77(22), 209, 213, 1996.

Bjorgo, E., O.M. Johannessen, and M.W. Miles. Analysis of merged SSMR-SSMI time series of Arctic and Antarctic sea ice parameters 1978-1995. *Geophys. Res. Lett.*, **24**(4), 413-416, 1997.

Budyco, M.I., Polar ice and climate. In Fletcher, J.O. (ed). Proceedings of the Symposium on the Arctic Heat Budget and Atmospheric Circulation, RM 5233-NSF, Rand Corporation, Santa Monica, CA, 3-21, 1966.

Carmack, E.C., R.W. Macdonald, R.G. Perkin, F.A. McLaughlin, and R.J. Pearson, Evidence

of warming of Atlantic Water in the southern Canadian Basin of the Arctic Ocean: Results from the Larson-93 expedition, Geophys. Res. Lett., 22, 1061-1064, 1995.

Comiso, J.C., Variability and trends in Antarctic surface temperatures from in situ and satellite infrared measurements, *J. Climate*, *13*(10), 1674-1696, 2000.

Comiso, J.C., Surface Temperatures in the Polar Regions using Nimbus-7 THIR, *J. Geophys. Res.*, *99*(C3), 5181-5200, 1994.

Comiso, J.C., and R. Kwok, The summer Arctic sea ice cover from satellite observations, *J. Geophys. Res.*, *101*(C2), 28397-28416, 1996.

Comiso, J.C., D. Cavalieri, C. Parkinson, and P. Gloersen, Passive microwave algorithms for sea ice concentrations, *Remote Sensing of the Env.*, *60*(3), 357-384, 1997.

Gloersen P., W. Campbell, D. Cavalieri, J. Comiso, C. Parkinson, H.J. Zwally, Arctic and Antarctic Sea Ice, 1978-1987: Satellite Passive Microwave Observations and Analysis, *NASA Spec. Publ.* 511, pp.290, 1992.

Honjo, S., T. Takizawa, R. Krishfield, J. Kemp, K. Hatekeyama, Drifting buoys make discoveries about interactive processes in the Arctic Ocean, *EOS Trans, AGU*, 76, 209, 215, 1995.

Jones, P. D., M. New, D. E. Parker, S. Martin, and I. G. Rigor, Surface air temperature and its changes over the past 150 years, *Rev. Geophys.*, **37**, 173– 199, 1999.

Krisfield, R., K. Doherty, and S. Honjo, Ice-Ocean Environmental Buoys (IOEB); Technology and deployment in 1991-1992, Technical Report WHOI-93-45, Woods Hole Oceanographic Institute, 86 pp., 1993.

Kwok, R., J.C. Comiso, and G. Cunningham, Seasonal characteristics of the perennial ice cover of the Beaufort Sea, *J. Geophys. Res.,101*(C2), 28417-28439, 1996.

Manabe, S., M. J. Spelman, and R. J. Stoufer, Transient responses of a coupled ocean-atmosphere model to gradual changes of atmospheric CO2. Part II: Seasonal response. *J. Climate*, 5, 105– 126, 1992.

Macdonald, R. W., E.C. Carmack, F.A. McLaughlin, K.K. Falkner, and J.H. Swift, Connections among ice, runoff, and atmospheric forcing in the Beaufort Gyre, *Geophys. Res. Lett., 26*(15), 2223-2226, 1999.

Maykut, G.A., and M.G. McPhee, Solar heating of the Arctic mixed layer, *J. Geophys. Res., 100,* 24,691-24,703, 1995.

Mcphee, M.G., T.P. Stanton, J.H. Morison, D.G. Martinson, Freshening of the upper ocean in the Arctic: Is perennial sea ice disappearing?, *Geophys. Res. Letter, 25*, 1729-1732, 1998.

Melling, H., Hydrographic changes in the Canada Basin of the Arctic Ocean, 1979-1996, *J. Geophys. Res., 103*(C4), 7637-7645, 1998.

Morison, J., M. Steele, and R. Anderson, Hydrography of the upper Arctic Ocean measured from the Nuclear Submarine USS Pargo, *Deep Sea Res., Part I, 45,* 15-38, 1998.

Mysak, L.A., Interannual variability at northern high latitudes, in: *Beyond El Nino: Decadal and*

interdecadal climate variability, ed. by A. Navarra, Springer-Verlag, 1-24, 1999.

Mysak, L.A., and S.A. Venegas, Decadal climate oscillations in the Arctic: A new feedback loop for atmosphere-ice-ocean interactions, *Geophys. Res. Lett., 25,* 19, 3607-3610, 1998.

Newton, J.L., B.J. Sotirin, Boundary undercurrent and water mass changes in the Lincoln Sea, *J. Geophys. Res., 102*(C2), 3393-3403, 1997.

Parkinson, C.L., D.J Cavalieri, P. Gloersen, H.J. Zwally, and J.C. Comiso, Arctic Sea ice extents, areas, and trends, 1978-1996. *J. Geophys. Res., 104*(C9), 20837-20856, 1999.

Perovich, D.K., B.C. Elder, J.A. Richter-Menge, Observations of the annual cycle of sea ice temperature and mass balance, *Geophys. Res. Lett. 24,* 555-558, 1997.

Proshutinsky, A. and M.Johnson, Two circular regimes of the wind driven Arctic Ocean, *J. Geophys. Res., 102,* 12,493-12,514, 1997.

Roach, A.T., K. Aagaard, C.H. Pease, S.A. Salo, T. Weingartner, V. Pavlov, and M. Kulakov, Direct measurements of transport and water properties through the Bering Sea, *J. Geophys. Res., 100*(C9), 18443-18457, 1995.

Rothrock, D. A., Y. Yu, and G. A. Maykut. 1999. Thinning of the Arctic sea-ice cover. *Geophys. Res. Letters*, *26*(23), 3469-3472.

Steffen, K., R. Bindschadler, C. Casassa, J. Comiso, D. Eppler, F. Fetterer, J. Hawkins, J. Key, D. Rothrock, R. Thomas, R. Weaver, and R. Welch. 1993. Snow and ice applications of AVHRR in Polar Regions. *Annals of Glaciology, 17,* 1– 16.

Steele, M., J.H. Morison, Hydrography and vertical fluxes of heat and salt northeast of Svalbard in autumn, *J. Geophys. Res., 98,* 10,013-10,024, 1993.

Thompson, D.W.J. and J.M. Wallace, The Arctic oscillation signature in the wintertime geopotential height and temperature fields, *Geophys. Res. Lett., 25,* 1297-1300, 1998.

Wadhams, P. 1988. Evidence of thinning of the Arctic ice cover north of Greenland. *Nature, 345*(6279), 795-797, 1988.

Wadhams, P. and N.R. Davis. Further evidence of ice thinning in the Arctic Ocean. *Geophys. Res. Letters, 27*(24), 3973 3976, 2000.

Yang, J., J.C. Comiso, R. Krishfield, and S. Honjo, The role of synoptic storms in the development of the 1997 warming and freshening event in the Beaufort Sea, *Geophys. Res. Lett., 27,* 2001.

List of Figures

July, September, and October of 1996, 1997, and 1998.

10. Yearly anomalies in ECMWF pressure maps from 1979 through 1999.

11. (a) Temperature and salinity profiles in 1996 and 1997; and (b) ice thickness change from 1996 to 1997.

12. T-S diagrams of daily temperature and salinity during each month (in red) at 8 m depth from April 1996 through December 1997 using IOEB data.

13. T-S diagrams of daily temperature and salinity during each month (in red) at 45 m depth from April 1996 through December 1997 using IOEB data.

14. T-S diagram of daily temperature and salinity during each month (in red) at 75 m depth from April 1996 through December 1997 using IOEB data.

15. (a) T-S diagrams of daily temperature and salinity during each month (in red) at 65 m depth from October 1997 through September 1998 using SHEBA IOEB data; and (b) T-S diagram of daily temperature and salinity during each month (in red) at 165 m depth from October 1997 through September 1998 using SHEBA IOEB data.

16. (a) Observed long term changes in monthly surface air temperature and 5 year running average and (b) the results of spectral analysis of a 5-year running mean of the data in (a).

17. Observed anomalies at 5 depths (10m, 40m, 70m, 110m, and 160m) in the Beaufort Sea from 1955 to 1998. EWG data were subtracted from data from T3/Arlis, Salargos, and IOES.

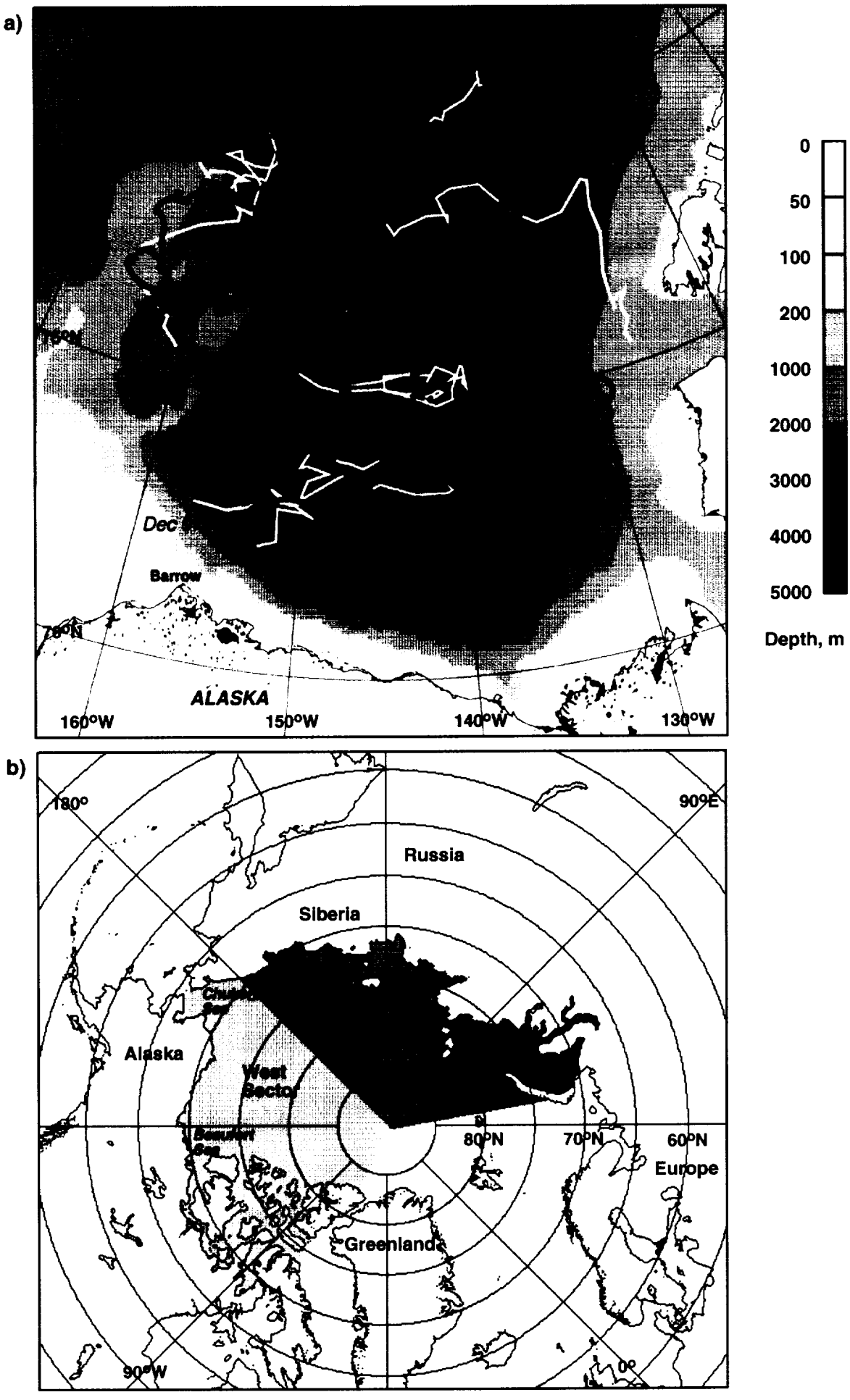
a)
Dec
Barrow
ALASKA
160°W
150°W
140°W
130°W
0
50
100
200
1000
2000
3000
4000
5000
Depth, m
b)
180°
90°E
Russia
Siberia
Alaska
West Sector
80°N
70°N
60°N
Europe
Greenland
90°W
0°

Fig 1

October 12, 1996

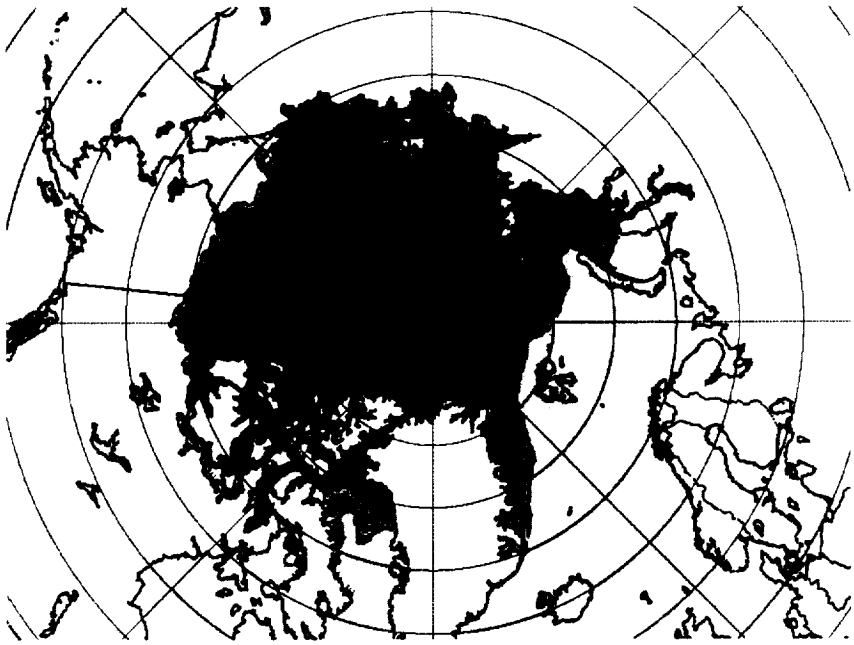

October 12, 1997

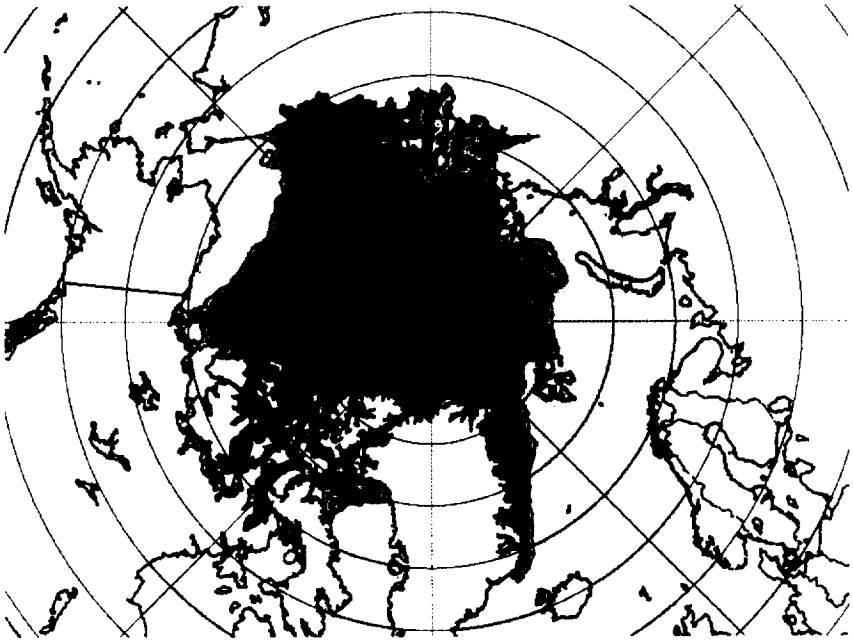

October 12, 1998

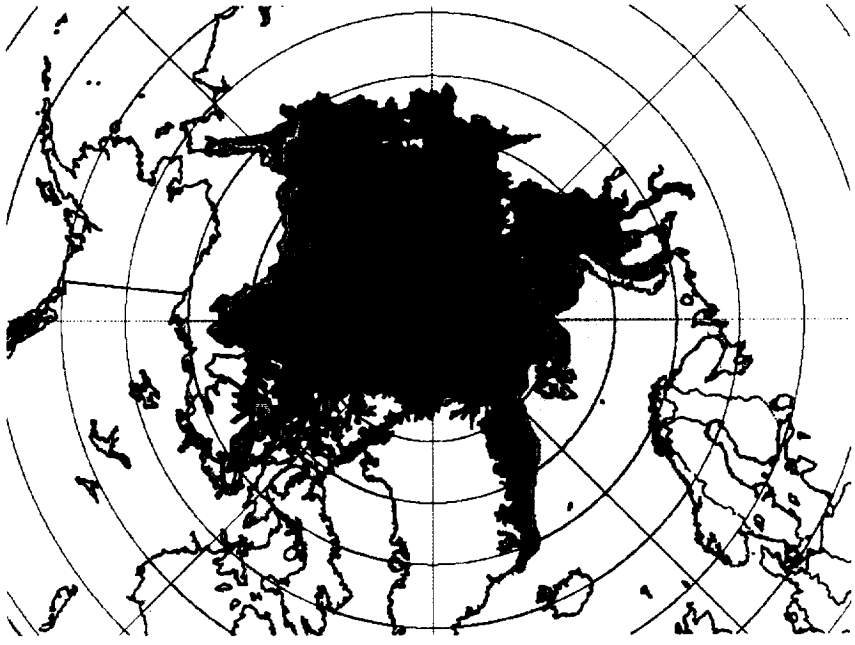

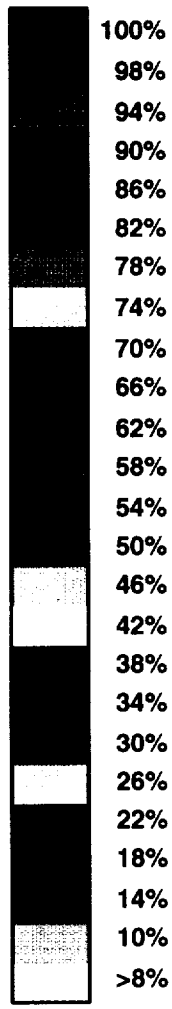

Fig 6

September Ice Concentration Anomalies

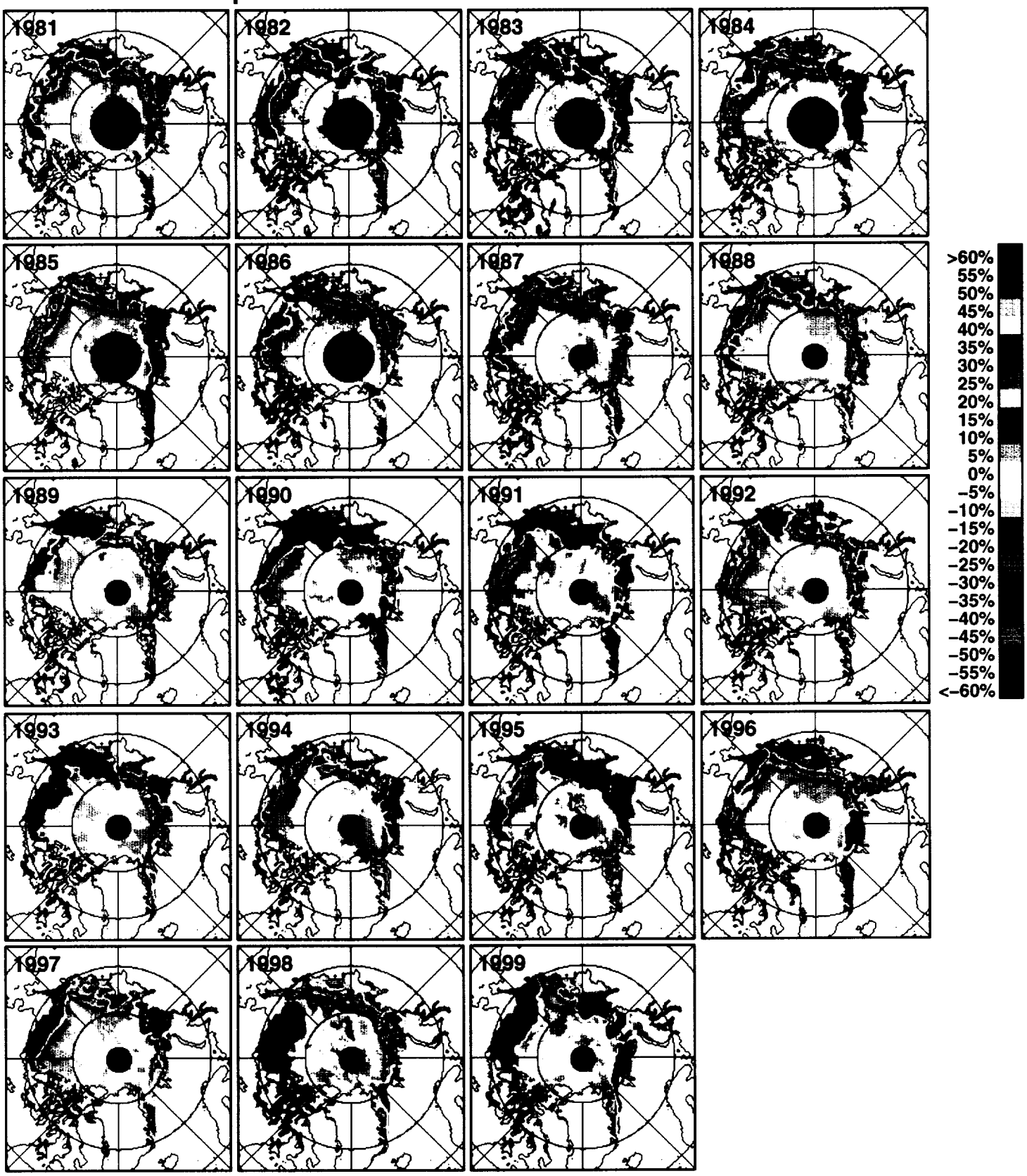

Northern Hemisphere Ice Cover

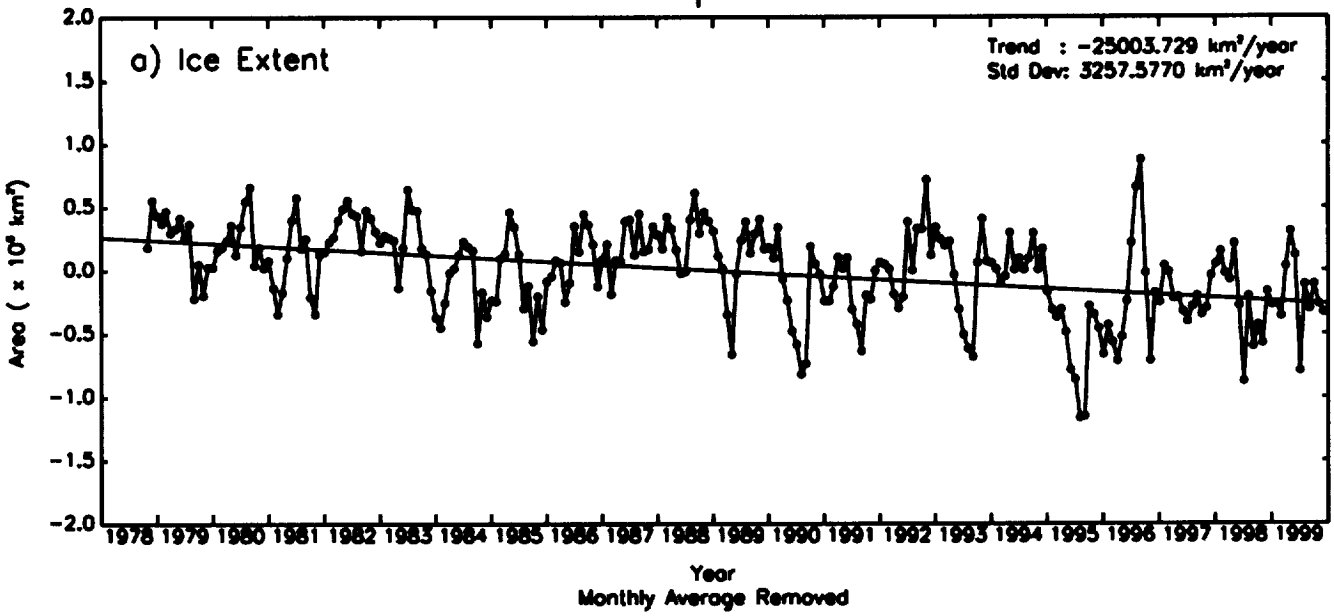

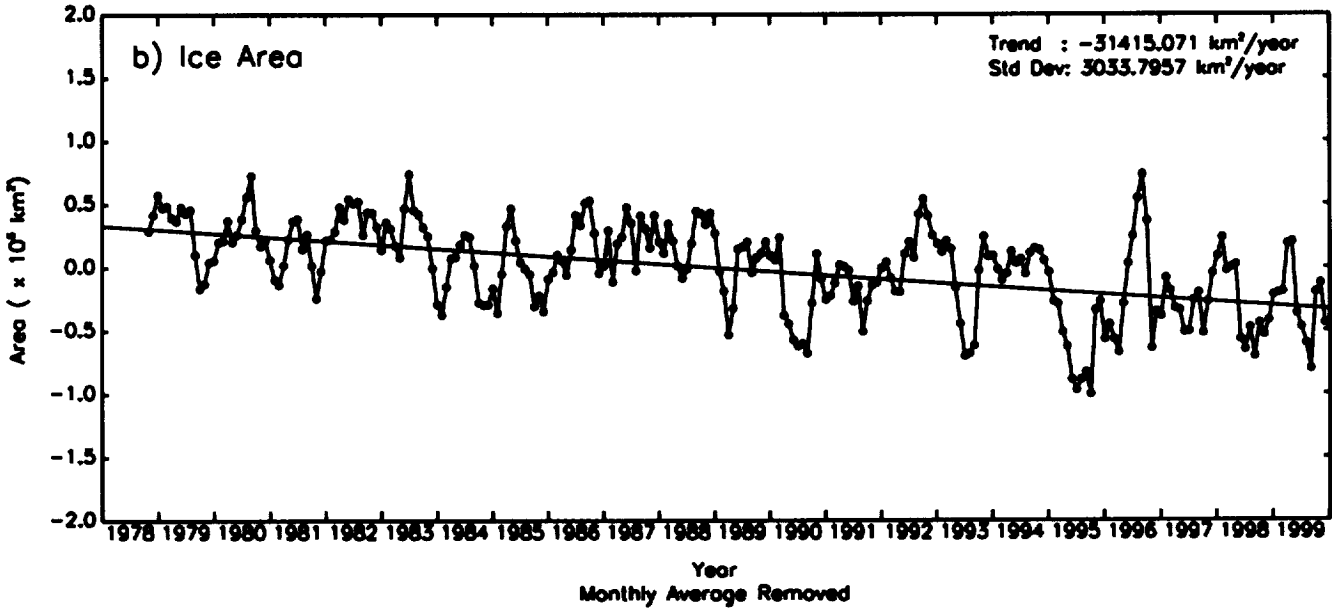

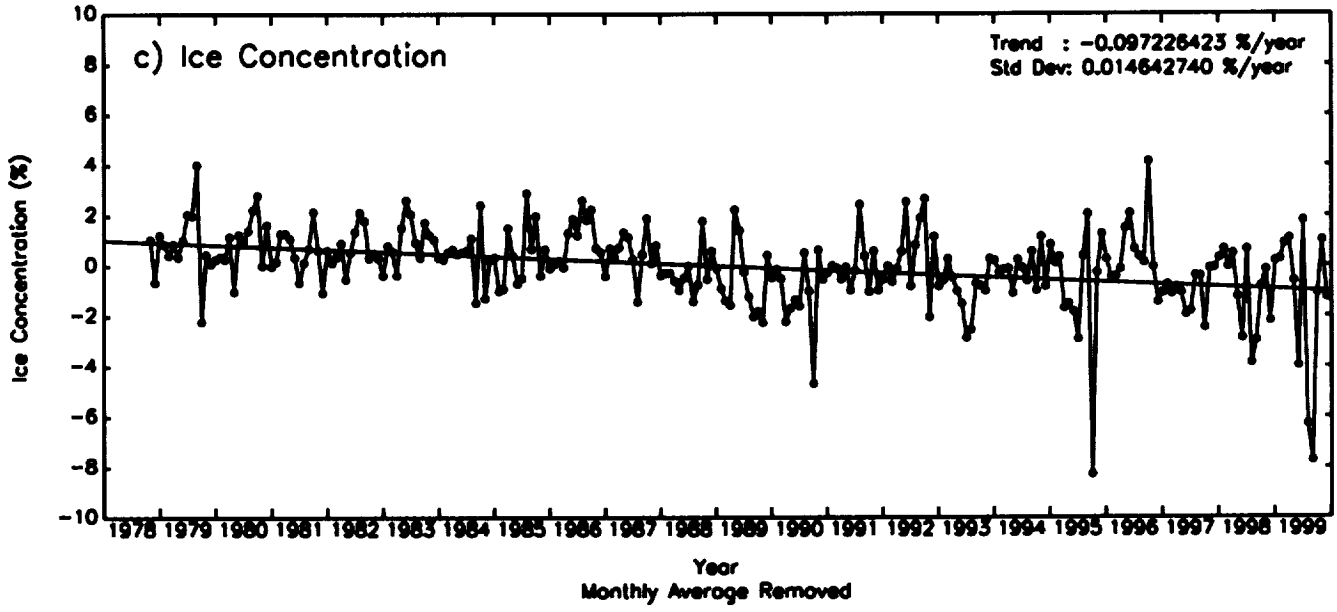

Arctic Open Water Area and Average Surface Temperatures

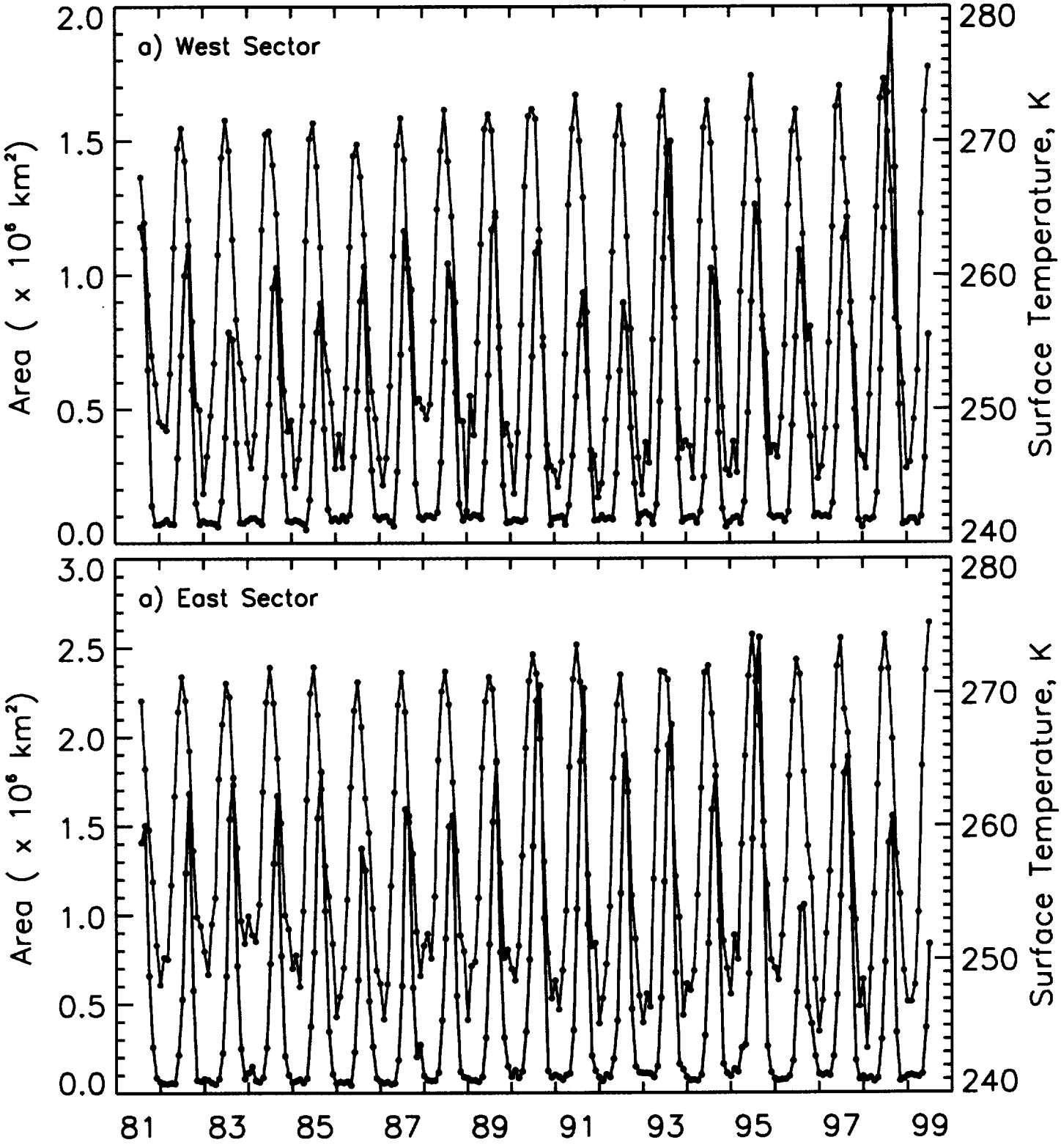

September Surface Temperature Anomalies

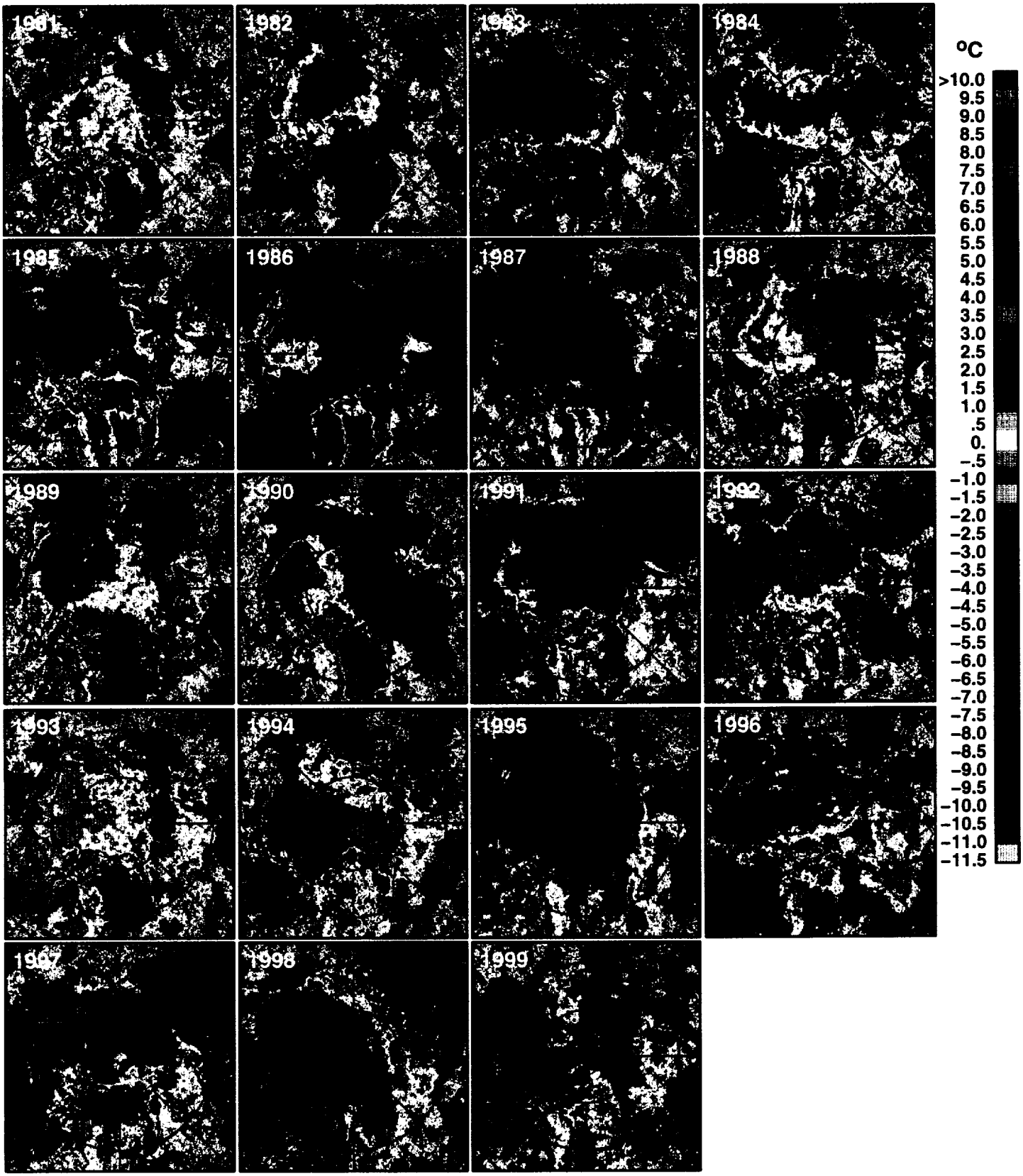

Anomalies in Surface Temperature

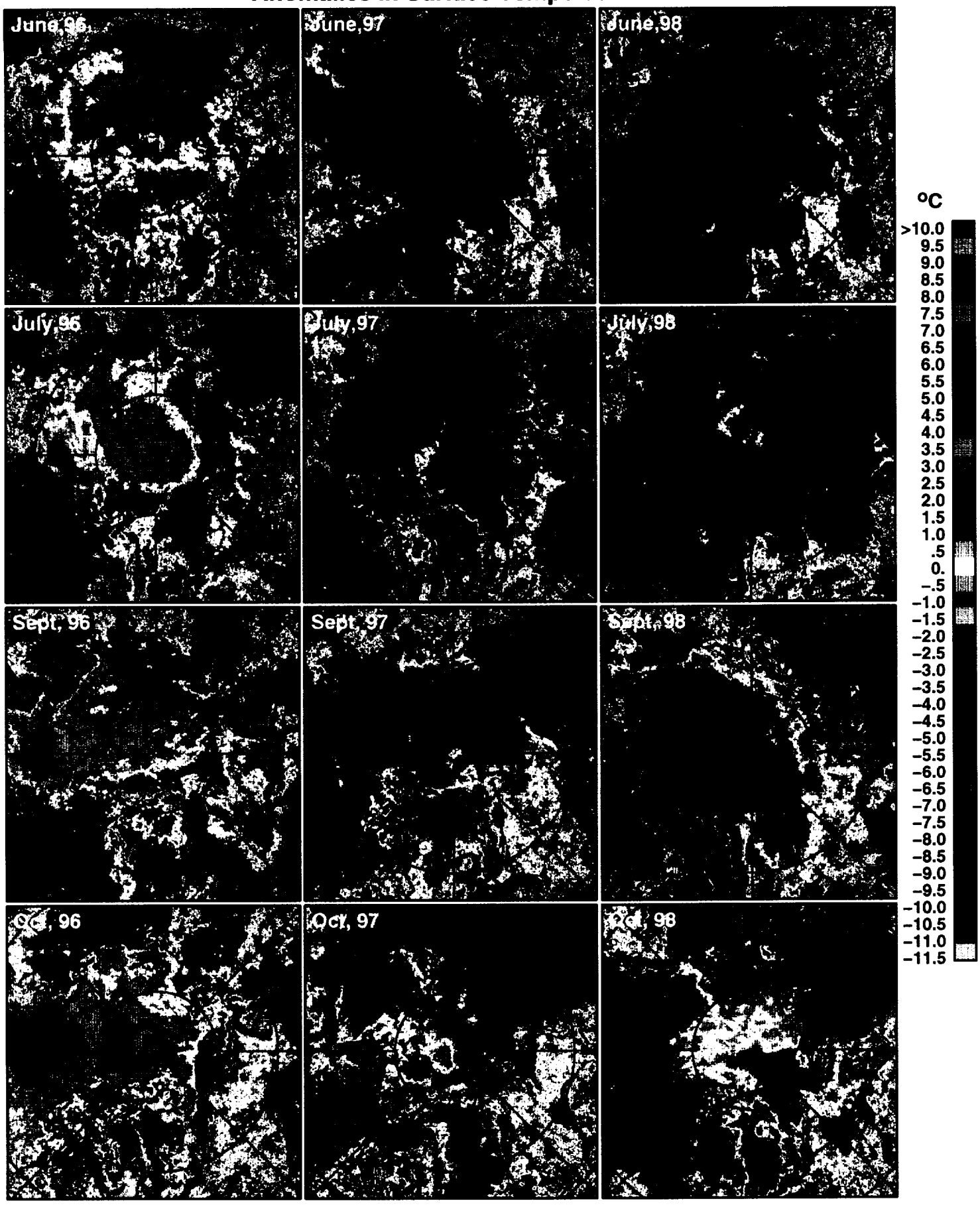

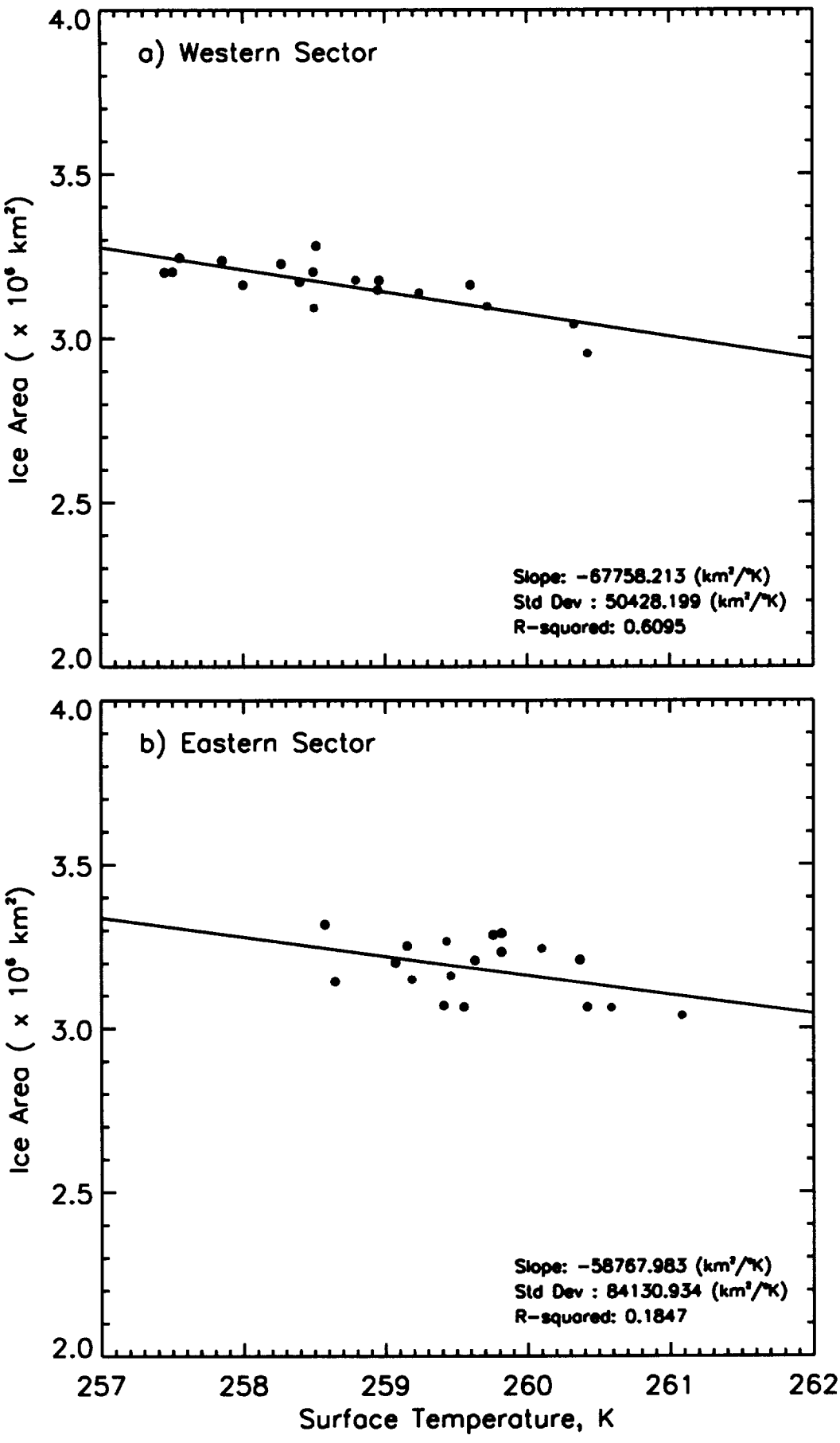

Color Key: Blue: 1981–1987
Green: 1987–1993
Orange: 1993–1999

Fig 2

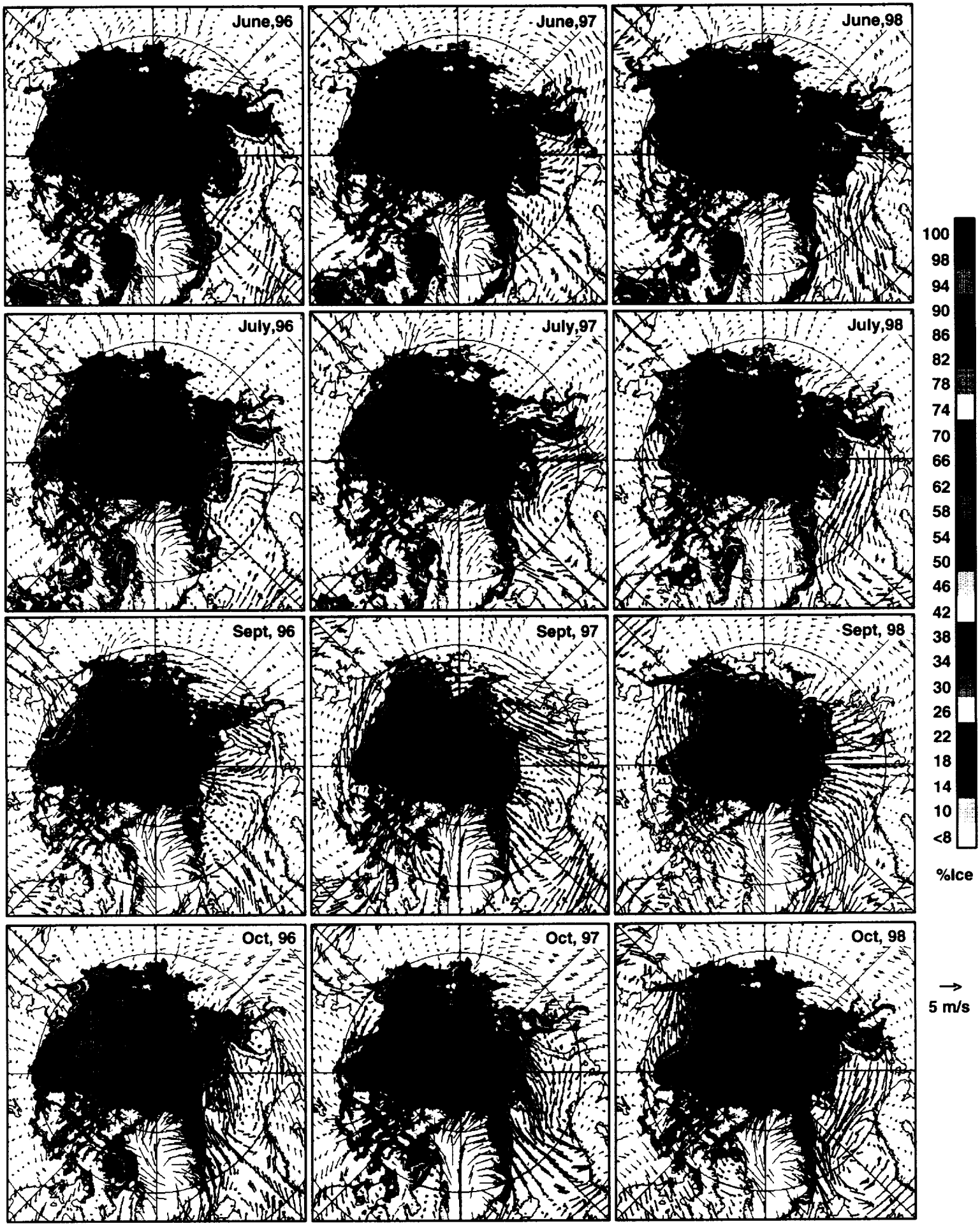
June,96
June,97
June,98
July,96
July,97
July,98
Sept, 96
Sept, 97
Sept, 98
Oct, 96
Oct, 97
Oct, 98
100
98
94
90
86
82
78
74
70
66
62
58
54
50
46
42
38
34
30
26
22
18
14
10
<8
%Ice
5 m/s

Fig 1

Summer MSL Pressure Anomalies

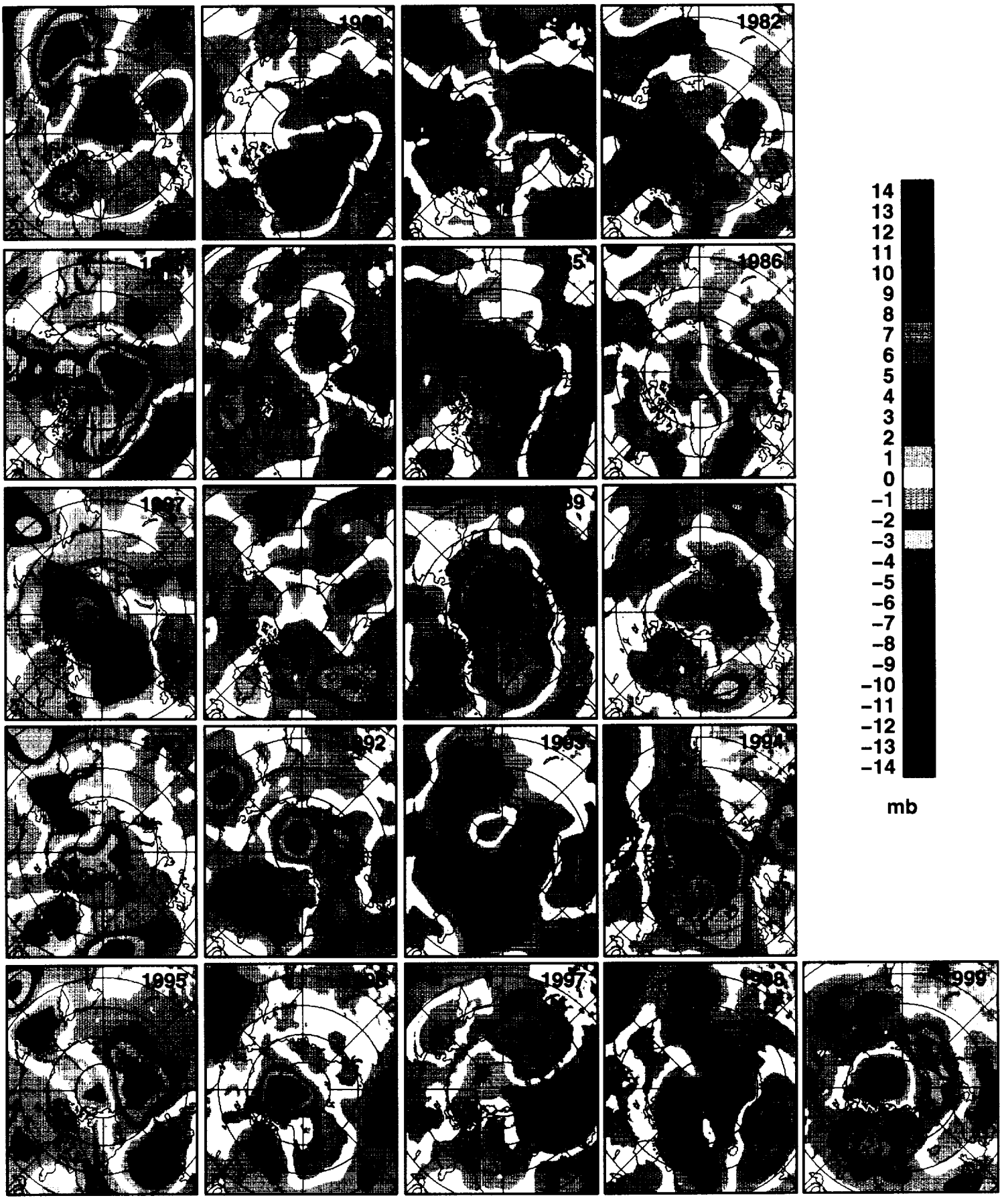

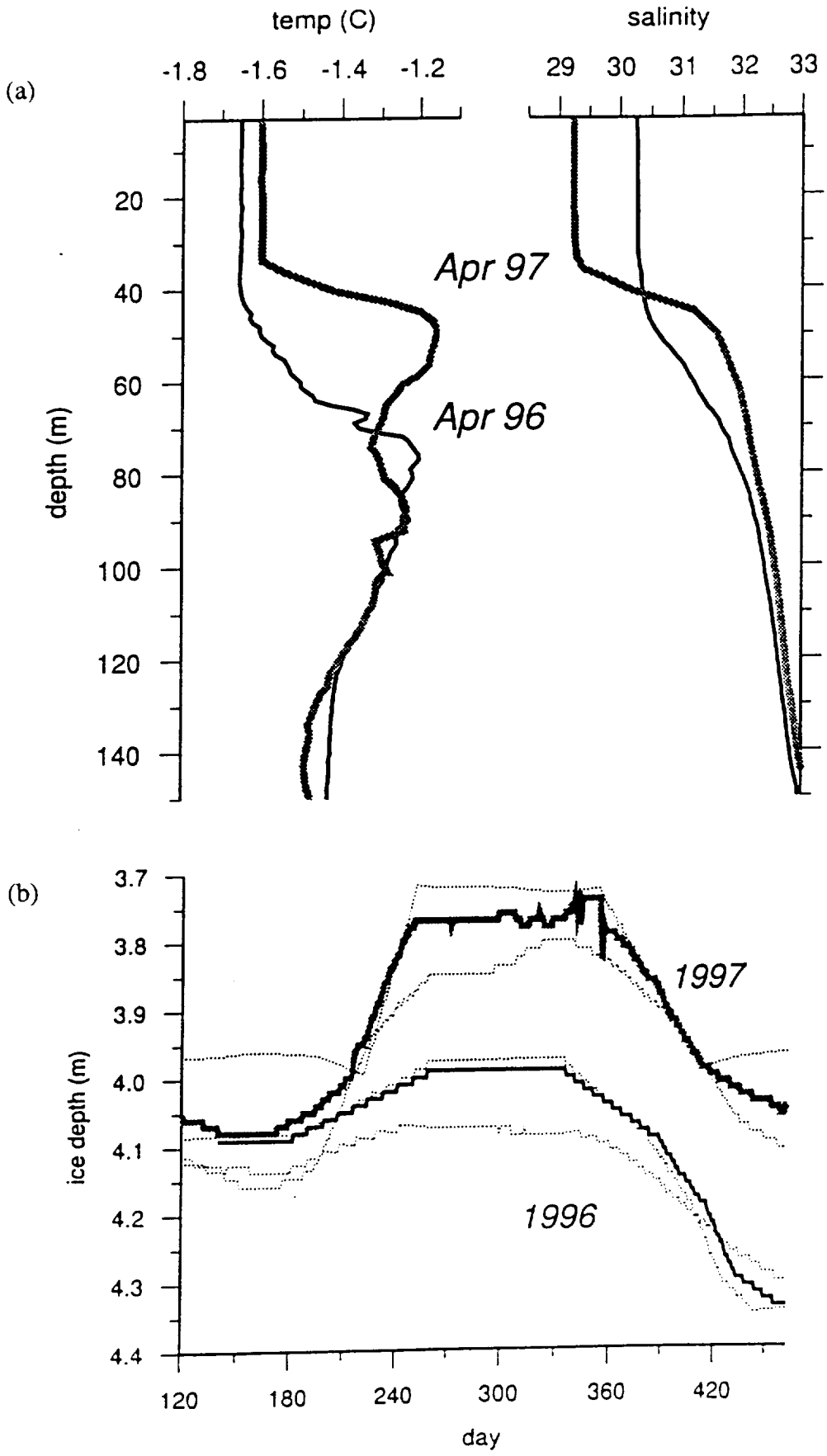
(a)
temp (C)
-1.8
-1.6
-1.4
-1.2
salinity
29
30
31
32
33
depth (m)
20
40
60
80
100
120
140
Apr 97
Apr 96
(b)
ice depth (m)
3.7
3.8
3.9
4.0
4.1
4.2
4.3
4.4
1997
1996
120
180
240
300
360
420
day

Fig. 11

IOEB BUOY DATA – DEPTH: ~8 m

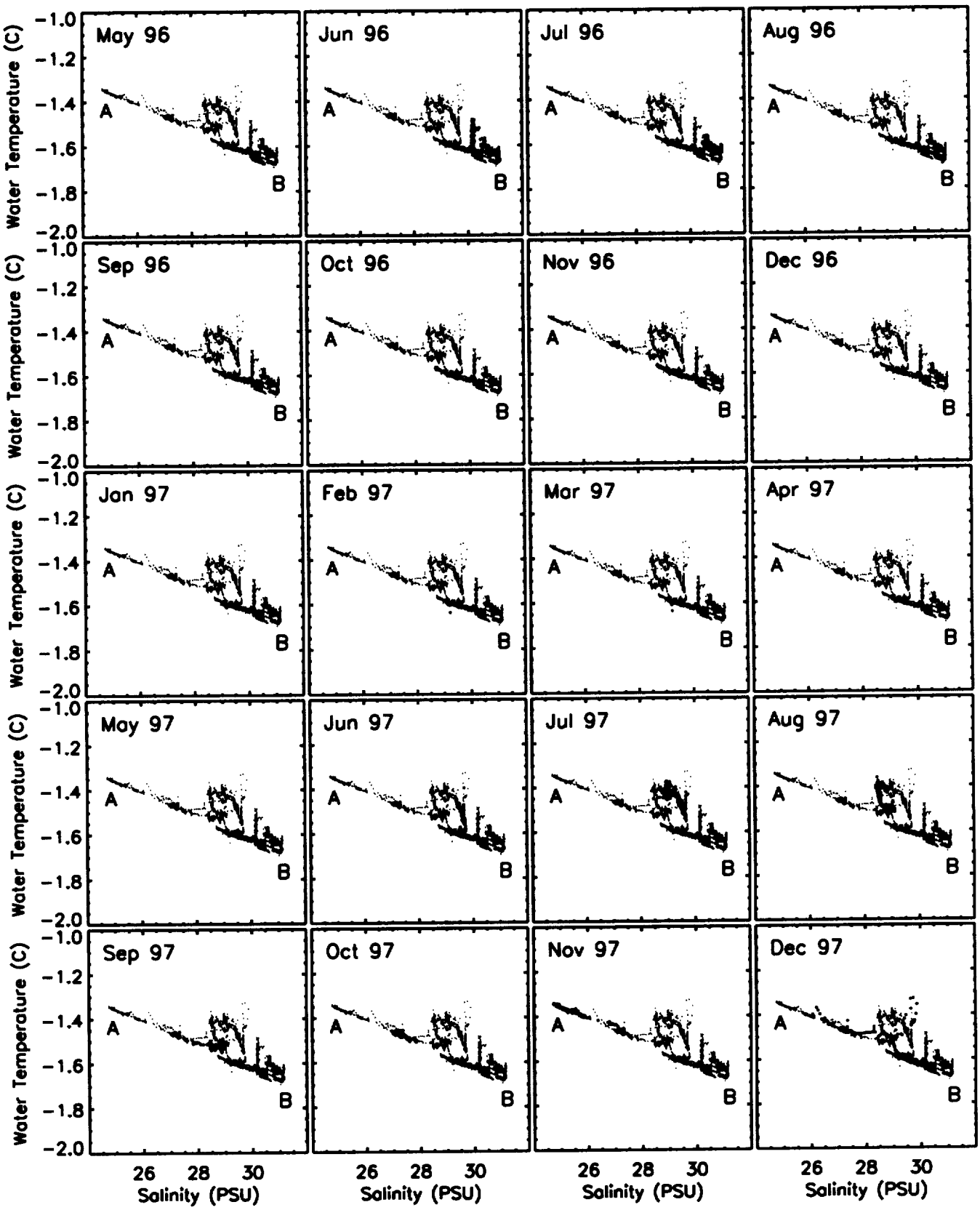

Fig 12

IOEB BUOY DATA – DEPTH: ~45 m

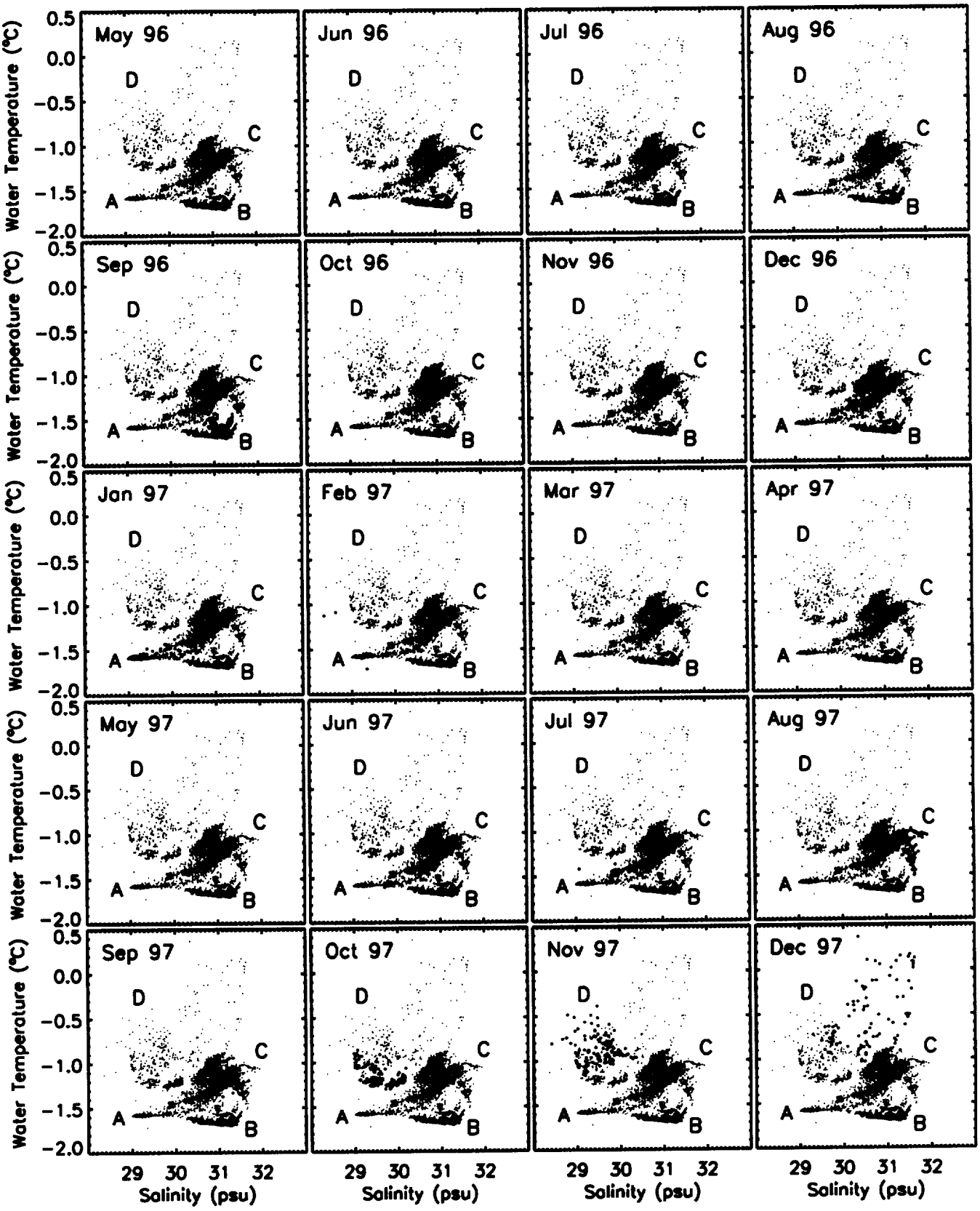

Fig 13

IOEB BUOY DATA – DEPTH: ~75 m

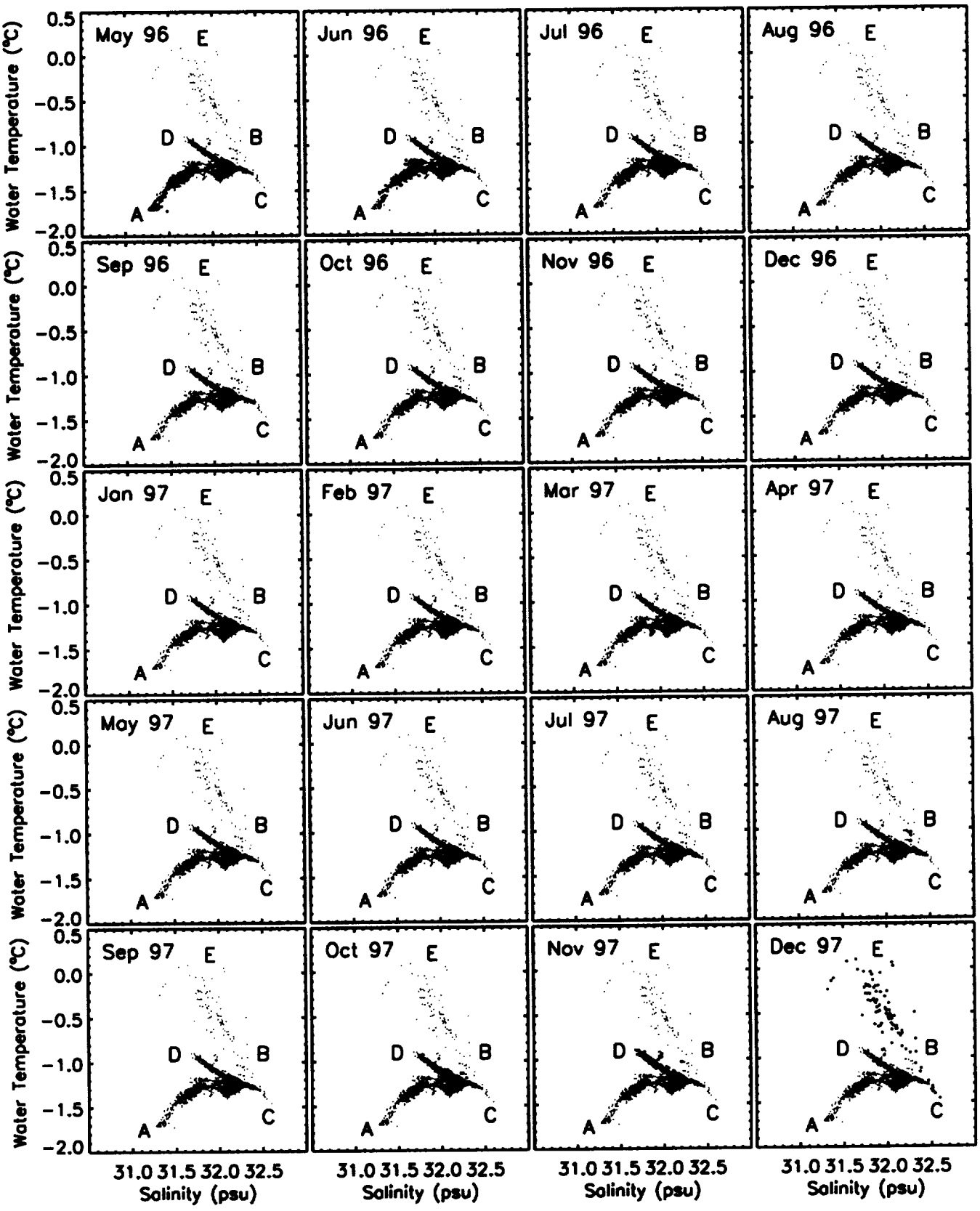

Fig 14

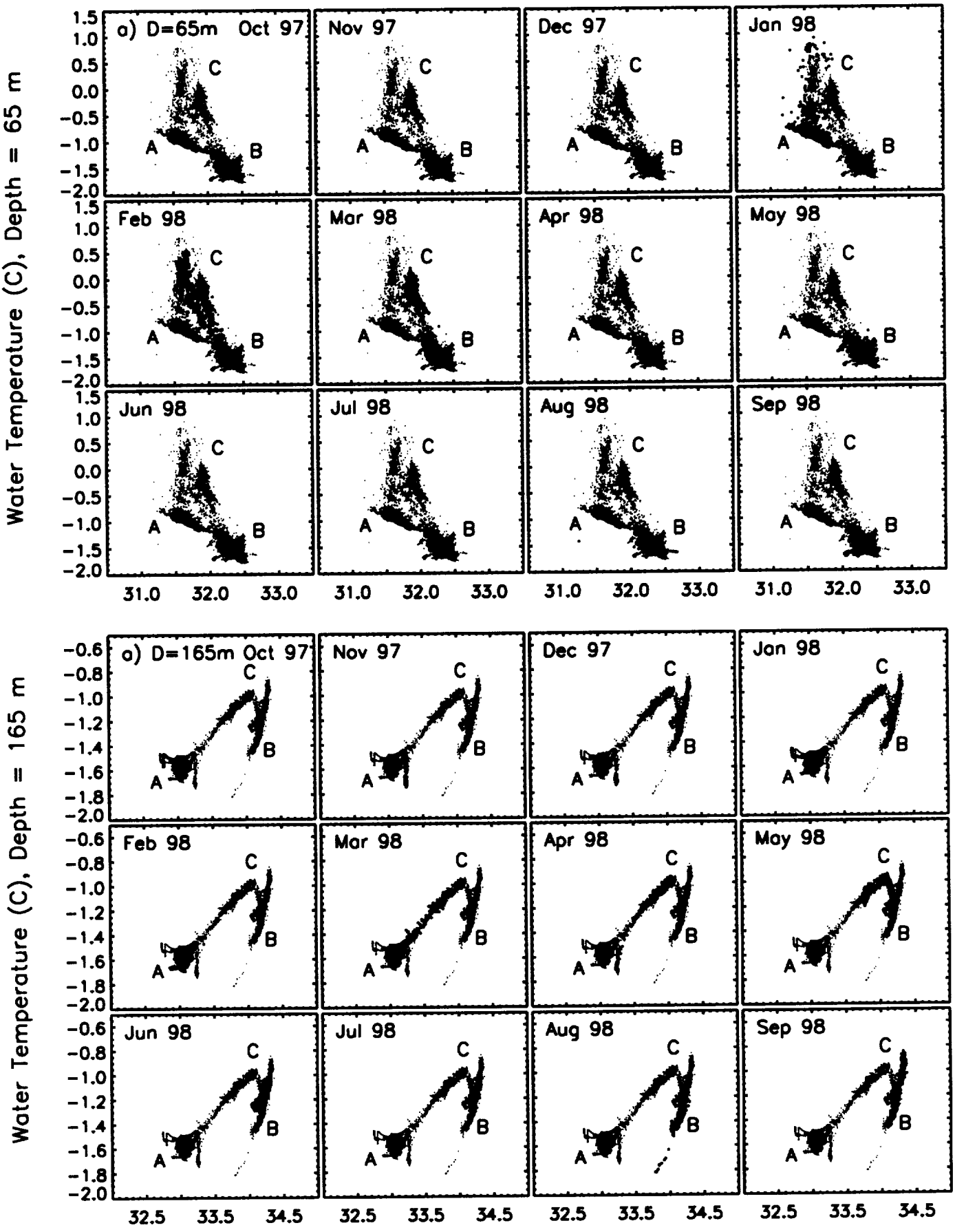
a) D=65m Oct 97
Nov 97
Dec 97
Jan 98
Feb 98
Mar 98
Apr 98
May 98
Jun 98
Jul 98
Aug 98
Sep 98
A
B
C
Water Temperature (C), Depth = 65 m
Water Temperature (C), Depth = 165 m
Salinity (PSU)

Fig 5

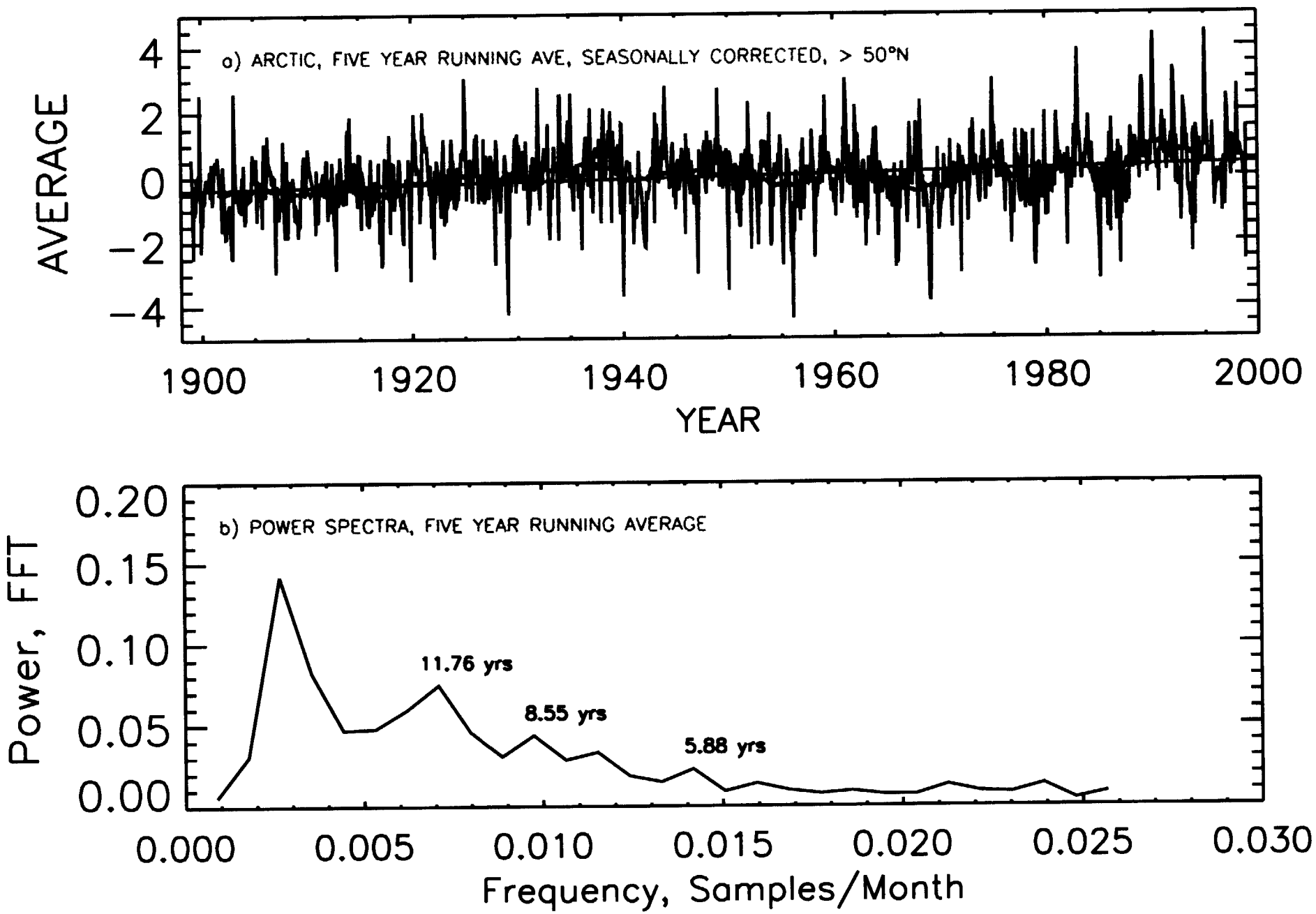
a) ARCTIC, FIVE YEAR RUNNING AVE, SEASONALLY CORRECTED, > 50°N
AVERAGE
4
2
0
−2
−4
1900
1920
1940
1960
1980
2000
YEAR
b) POWER SPECTRA, FIVE YEAR RUNNING AVERAGE
Power, FFT
0.20
0.15
0.10
0.05
0.00
11.76 yrs
8.55 yrs
5.88 yrs
0.000
0.005
0.010
0.015
0.020
0.025
0.030
Frequency, Samples/Month

Fig 16

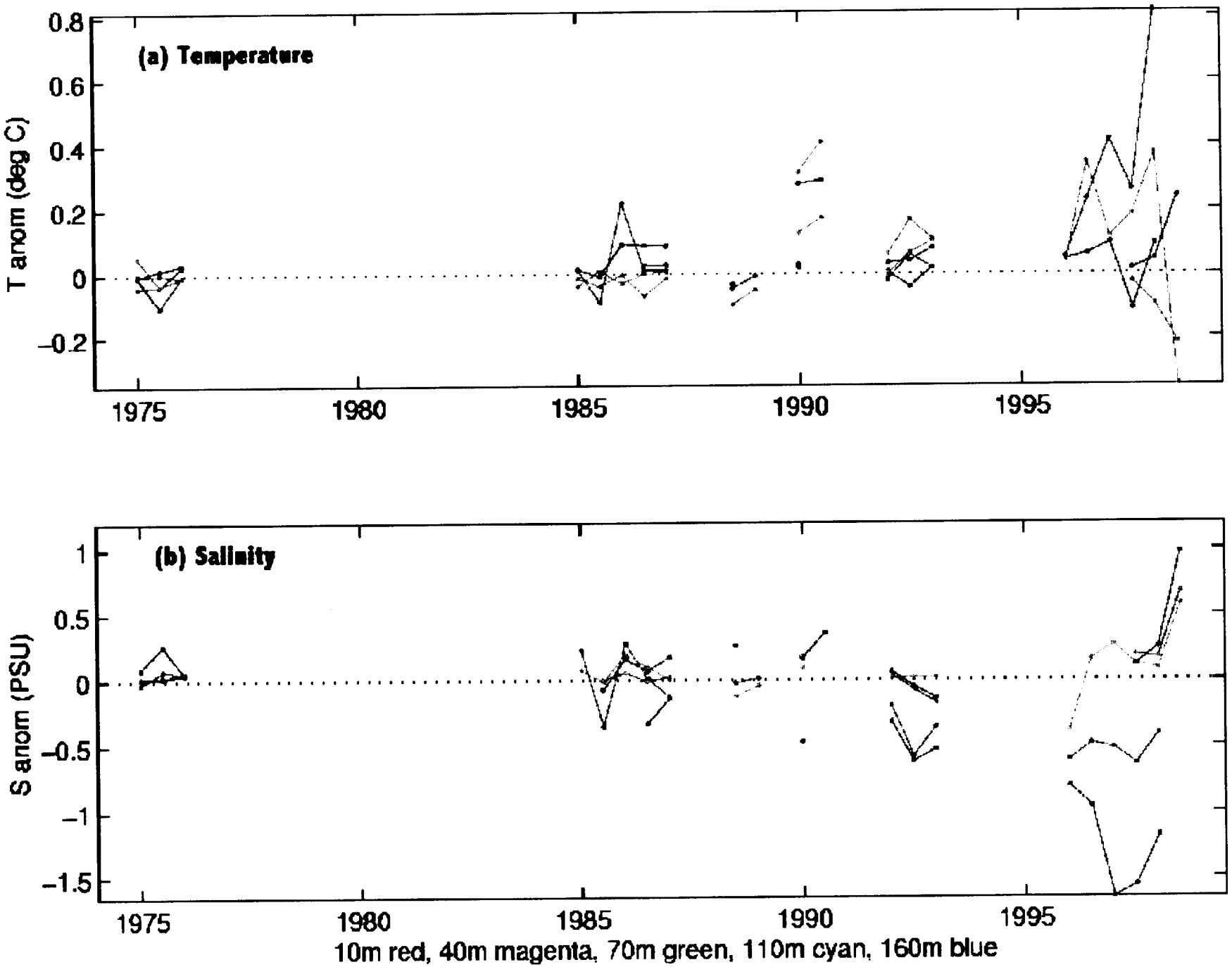
(a) Temperature
T anom (deg C)
0.8
0.6
0.4
0.2
0
−0.2
1975
1980
1985
1990
1995
(b) Salinity
S anom (PSU)
1
0.5
0
−0.5
−1
−1.5
1975
1980
1985
1990
1995
10m red, 40m magenta, 70m green, 110m cyan, 160m blue